Antiproton-proton partial-wave analysis below 925 MeV/c

R. Timmermans,* Th.A. Rijken, and J.J. de Swart
Institute for Theoretical Physics, University of Nijmegen, Nijmegen, The Netherlands
(Received 30 September 1993)

A partial-wave analysis of all $\bar{p}p$ scattering data below 925 MeV/c antiproton laboratory momentum is presented. The method used is adapted from the Nijmegen phase-shift analyses of pp and np scattering data. We solve the Schrödinger equation for the coupled $\bar{p}p$ and $\bar{n}n$ channels where the long- and intermediate-range interactions are described by a theoretically well-founded potential. This gives the rapid variations of the scattering amplitudes with energy. This potential consists of the Coulomb potential with the main relativistic correction, the magnetic-moment interaction, the one-pion-exchange potential, and the heavy-boson exchanges of the Nijmegen one-boson-exchange potential. Slow variations of the amplitudes due to short-range interactions, including the coupling to mesonic annihilation channels, are parametrized by an energy-dependent, complex boundary condition, specified at a radius of $r = 1.3$ fm. The Nijmegen 1993 $\bar{p}p$ database, consisting of 3646 $\bar{p}p$ scattering data, is presented and discussed. The best fit to this database results in $\chi^2_{\min}/N_{\text{data}} = 1.043$. This good fit to the data shows that the Nijmegen long- and intermediate-range potential is essentially correct. The pseudovector coupling constant of the charged pion to nucleons is determined to be $f_c^2 = 0.0732(11)$ at the pion pole, where the error is statistical.

PACS number(s): 13.75.Cs, 11.80.Et

I. INTRODUCTION

A partial-wave analysis (PWA) of all antiproton-proton ($\bar{p}p$) scattering data below antiproton laboratory momentum $p_{\text{lab}} = 925$ MeV/c is presented. In the field of nucleon-nucleon (NN) scattering, phase-shift analyses (more properly called partial-wave analyses, PWA's) have a long history and at present the multienergy or energy-dependent partial-wave analyses of NN scattering data have reached a stage of considerable sophistication [1–7]. Due to the poor quality of low-energy antiproton beams and the resulting absence of accurate experimental data, analogous model-independent studies of the much more complex $\bar{p}p$ system have in the past always been impossible.

In recent years, however, experimental progress has been very significant, in particular due to the advent in 1983 of the LEAR facility at CERN. In the momentum region that we consider in the analysis presented in this paper, the situation between 400 and 925 MeV/c is quite good: a variety of observables have been measured with impressive accuracy. However, the practical difficulties involved in constructing a high-quality antiproton beam of even lower momentum are large. As a result, the $\bar{p}p$ database below about 400 MeV/c is still by far not as good as one would like [8–10], in contrast to the case of NN scattering, where for instance very accurate proton-proton differential cross sections have been taken at energies as low as $T_{\text{lab}} = 0.35$ MeV ($p_{\text{lab}} = 25.6$ MeV/c).

During the last 10 years a new method has been developed by the Nijmegen group to perform partial-wave analyses of the NN (proton-proton and neutron-proton) scattering data below laboratory kinetic energy $T_{\text{lab}} = 350$ MeV ($p_{\text{lab}} = 883$ MeV/c). The hallmark of this method is that the theoretical knowledge of the NN interaction is exploited as much as possible in the description of the energy dependence of the partial-wave scattering amplitudes. This is done by solving the relativistic Schrödinger equation for each partial wave and at each energy with the theoretically well-known long-range NN interaction represented by the potential for $r > b = 1.4$ fm. This long-range interaction is responsible for the fast variation with energy of the scattering amplitudes. The much slower energy variations of the amplitudes due to the short-range interactions are parametrized phenomenologically by the energy dependence of a boundary condition at $r = b$. In this way one also avoids the complications due to the lack of knowledge of this short-range interaction. In order to achieve a good fit to the NN data one has to include in the long-range interaction the complete electromagnetic interaction (including relativistic and some two-photon-exchange effects, the magnetic-moment interactions, and the vacuum-polarization potential), the one-pion-exchange potential, and also the intermediate-range forces (due to two-pion exchange and/or heavier-meson exchange) of some realistic NN potential model.

The dominant feature of $\bar{p}p$ scattering at low energies is the annihilation into mesons, a process that has no counterpart in NN scattering. Annihilation is, in principle, a very complicated spin-, isospin-, and energy-dependent multiparticle process. At rest, where kinematically the production of 13 neutral pions is allowed, 5 pions are produced on the average [11], and of the order of 100

---

*Present address: Theoretical Division, Mail Stop B283, Los Alamos National Laboratory, Los Alamos, NM 87545. Electronic address: timmer@t5zia.LANL.GOV

two-meson channels contribute significantly [12,13]. In recent years some progress has been made in understanding specific annihilation processes in terms of quark-gluon degrees of freedom. However, for the description of elastic $\bar{p}p \to \bar{p}p$ and charge-exchange $\bar{p}p \to \bar{n}n$ scattering, only a phenomenological approach to annihilation is feasible at present. In potential models for antinucleon-nucleon $(\overline{NN})$ scattering one usually simplifies things drastically by taking the annihilation potential to be completely independent of spin, angular momentum, isospin, and energy. This assumption is implemented either by applying a simple absorptive boundary condition [14–17], or by using a state-independent two- or three-parameter optical potential [18–23]. However, when one is interested in describing the data quantitatively, including spin-dependent observables, a less naive approach is called for. For instance, in the Paris $\overline{NN}$ model [24,25] a spin-, isospin-, and energy-dependent optical potential is employed, and in the Nijmegen coupled-channels model [26] each $\overline{NN}$ channel is coupled to two effective two-body mesonic channels (for the coupled-channels approach see also Ref. [27]). In both cases of the order of 15 parameters were needed to obtain a more or less satisfactory fit to the pre-LEAR data, the bulk of which consisted of elastic differential cross sections. At that time charge-exchange data and spin-dependent observables were practically absent. Because the $\overline{NN}$ system is so much more complicated than the already quite complex NN system it was then believed that it would be impossible to perform a PWA of the $\bar{p}p$ scattering data.

The complexity of the $\bar{p}p$ system when compared to the NN system (below the pion-production threshold) is reflected in the following manner in a PWA. In proton-proton (pp) scattering (isospin $I = 1$) one has to specify at each energy two phase shifts ($^1S_0$ and $^3P_0$) for $J = 0$ and on the average 2.5 phase parameters for each value of the total angular momentum $J \neq 0$. As an example, for $J = 1$ one needs only one phase shift ($^3P_1$), while for $J = 2$ one needs four phase parameters (the $^1D_2$, $^3P_2$, and $^3F_2$ phase shifts and the ε_2 mixing parameter). In a PWA of the neutron-proton (np) scattering data (both isospin $I = 0$ and $I = 1$) again two phase shifts are required for $J = 0$, but now five phase parameters are required for each value of $J \neq 0$. Due to the lack of sufficient high-quality np data it has been impossible to do a good PWA of the np data alone. One needs to take the $I = 1$ phases (with the exception of the $^1S_0$ phase shift) from the PWA of the pp data and correct them for electromagnetic and mass-difference effects (M_p versus M_n and m_{π^0} versus $m_{\pi^\pm}$). In the case of $\bar{p}p$ scattering the Pauli principle is not operative. Apart from this, the possibility for the $\bar{p}p$ system to annihilate into mesons complicates things even further. This means that one has to determine no less than four times as many phase parameters compared to the case of np scattering, so eight phase parameters are required for $J = 0$ and 20 phase parameters for each value of $J \neq 0$. In view of this, the situation with regards to a $\bar{p}p$ PWA indeed seemed quite hopeless.

Using essentially the same strategy as in the Nijmegen multienergy partial-wave analyses of NN scattering data, and with the available recent high-quality data from LEAR and KEK, we have nevertheless been able to perform a PWA of $\bar{p}p$ scattering data below 925 MeV/c. This work was started in 1987 [28] and a preliminary report of this analysis has already been given [29]. The Schrödinger equation for the coupled antiproton-proton and antineutron-neutron $(\bar{n}n)$ channels is solved. The short-range interaction, including the coupling to the mesonic annihilation channels, is parametrized by way of a complex boundary condition specified at $r = b = 1.3$ fm. The long-range interaction consists of the Coulomb potential, the magnetic-moment interaction, and the one-pion-exchange potential. The tail of the heavy-boson-exchange part of the Nijmegen potential [30] is used as intermediate-range interaction. A lot of time and effort has gone into collecting, scrutinizing, and cleaning up the world set of $\bar{p}p$ scattering data, which contains quite some flaws and contradictory data. Exactly the same arguments were used in this process as were used in the setup of the Nijmegen NN database [5–7]. The resulting Nijmegen 1993 $\bar{p}p$ database in the momentum interval 119–923 MeV/c consists of $N_{\text{data}} = 3646$ $\bar{p}p$ data, which can be fitted with $\chi^2_{\text{min}}/N_{\text{data}} = 1.043$. In view of the excellent quality of this fit one can be confident that most of the amplitudes are quite well described. The same methods have also been applied by us to the strangeness-exchange reaction $\bar{p}p \to \overline{\Lambda}\Lambda$, which is an even more complicated process [31,32].

This paper is organized as follows. In Sec. II we present the details of the method of analysis. In Sec. III the treatment of the short-range interaction by parametrizing an energy-dependent boundary condition is discussed. In Sec. IV the long-range electromagnetic and pion-exchange potential are presented and we specify the heavy-meson exchanges used as intermediate-range interaction. In Sec. V we discuss the nontrivial problem how to extract the nuclear scattering amplitude in the presence of electromagnetic effects. The definition of the phase-shift and mixing parameters for antinucleon-nucleon scattering can be found in Sec. VI. The statistical tools used in the analysis are briefly reviewed in Sec. VII. In Sec. VIII the Nijmegen 1993 antiproton-proton database is extensively discussed. Next, in Sec. IX we present the results of the analysis, including the determination of the pion-nucleon coupling constant. The most important results and conclusions are summarized in Sec. X. The algorithm to extract the phase parameters from the S matrix is reviewed in the Appendix.

II. THE METHOD OF ANALYSIS

The two-body scattering process is described with the coupled-channels relativistic Schrödinger equation

$$[\Delta + p^2 - 2mV]\,\psi(\mathbf{r}) = 0 \ . \tag{1}$$

This is a matrix equation in channel space. We use the physical particle basis $\bar{p}p$, $\bar{n}n$ in order to treat electromagnetic effects properly and to account for the threshold of charge-exchange scattering $\bar{p}p \to \bar{n}n$ at $p_{\text{lab}} = 99.1$ MeV/c ($T_{\text{lab}} = 5.2$ MeV). The connection between the

channel momentum p and the total energy $\sqrt{s}$ in the center-of-mass system is given by the relativistic expression $p^2 = \frac{1}{4}s - m^2$ (for equal masses). The relativistic Schrödinger equation (1) is a differential form of the relativistic Lippmann-Schwinger integral equation [33,34]. The difference between the relativistic and the ordinary nonrelativistic Lippmann-Schwinger equation [35] is the relation used between energy and momentum. The relativistic Lippmann-Schwinger equation is in turn equivalent to three-dimensional relativistic integral equations like the Blankenbecler-Sugar equation [36–39]. For a discussion about the derivation of potentials for use in the relativistic Schrödinger equation, starting from the field-theoretical Bethe-Salpeter equation [40,41], see for instance Refs. [42,43].

The interaction in the region $r > b$ is described by a theoretically well-founded antinucleon-nucleon potential. This potential is given by

$$V = V_C + V_{\mathrm{MM}} + V_N , \tag{2}$$

where V_C and V_{MM} are the relativistic Coulomb and magnetic-moment interaction respectively. V_N is the $\overline{N}N$ meson-exchange potential. The precise forms of these potentials are discussed in Sec. IV. After making the partial-wave projection by writing

$$\psi(\mathbf{r}) = \sum_{\ell s J m} \Phi_{\ell s J}^m(r)/r \; \mathcal{Y}_{\ell s J}^m(\theta) , \tag{3}$$

where

$$\mathcal{Y}_{\ell s J}^m(\theta) = \sum_{m_\ell m_s} C_{m_\ell \; m_s \; m}^{\ell \; s \; J} \, Y_{m_\ell}^\ell(\theta) \, \xi_m^s , \tag{4}$$

we obtain the radial Schödinger equation, which for partial waves with total angular momentum J reads

$$\left[\frac{d^2}{dr^2} - \frac{L^2}{r^2} + p^2 - 2mV^J \right] \Phi^J(r) = 0 . \tag{5}$$

V^J is now a matrix with elements $\langle \ell' s' a' | V^J(r) | \ell \, s \, a \rangle$, where a is an index used to distinguish the different channels. For partial waves with $\ell = J$, $s = 0, 1$ all matrices are 2×2, and for waves with $\ell = J \pm 1$, coupled by the tensor force, they are 4×4. The Schrödinger equation is solved numerically [44] starting with the boundary condition at $r = b$ and ending at a value r_∞ beyond the range of the nuclear potential. At this point the S matrix is obtained by matching this numerical solution Φ to the required asymptotic form

$$\Phi_{\mathrm{as}}(r) \overset{r \to \infty}{\sim} \sqrt{\frac{m}{p}} \left[H_2(pr) + H_1(pr) S^J \right] . \tag{6}$$

Since the Coulomb potential has infinite range one has to match to Coulomb wave functions, so H_1 and H_2 are diagonal matrices with entries $H_\ell^{(1)}(\eta_a, p_a r)$ and $H_\ell^{(2)}(\eta_a, p_a r)$, the Coulomb analogues of the spherical Hankel functions. η_a is the relativistic Coulomb parameter

$$\eta_a = \alpha/v_{\mathrm{lab}} = \alpha' m_a/p_a . \tag{7}$$

Written in terms of the standard regular and irregular Coulomb wave functions, $F_\ell(\eta, pr)$ and $G_\ell(\eta, pr)$, these Hankel functions are defined as

$$H_\ell^{(1)}(\eta_a, p_a r) = F_\ell(\eta_a, p_a r) - iG_\ell(\eta_a, p_a r), \quad H_\ell^{(2)}(\eta_a, p_a r) = F_\ell(\eta_a, p_a r) + iG_\ell(\eta_a, p_a r) . \tag{8}$$

These Coulomb wave functions read asymptotically

$$F_\ell(\eta_a, p_a r) \overset{r \to \infty}{\sim} \sin \left[p_a r - \ell \frac{\pi}{2} + \sigma_{\ell, a} - \eta_a \ln(2 p_a r) \right] , \tag{9}$$

$$G_\ell(\eta_a, p_a r) \overset{r \to \infty}{\sim} \cos \left[p_a r - \ell \frac{\pi}{2} + \sigma_{\ell, a} - \eta_a \ln(2 p_a r) \right] , \tag{10}$$

where the Coulomb phase shifts $\sigma_{\ell, a}$ are given by

$$\sigma_{\ell, a} = \arg \Gamma(\ell + 1 + i\eta_a) . \tag{11}$$

In case the Coulomb interaction is absent in a channel (like $\bar{n}n$), one can simply put $\eta_a = 0$. Then the Coulomb wave functions become

$$F_\ell(0, \rho) = \rho j_\ell(\rho), \quad G_\ell(0, \rho) = -\rho n_\ell(\rho) ,$$

$$H_\ell^{(1)}(0, \rho) = \rho h_\ell^{(1)}(\rho), \quad H_\ell^{(2)}(0, \rho) = \rho h_\ell^{(2)}(\rho) , \tag{12}$$

in terms of ordinary spherical Bessel, Neumann, and Hankel functions. The matching procedure at r_∞ works

as follows. The multichannel Wronskian is defined by

$$W(\Phi_1, \Phi_2) = \Phi_1^T \frac{1}{m} \Phi_2' - \Phi_1'^T \frac{1}{m} \Phi_2 , \tag{13}$$

where the prime denotes differentiation with respect to r and the "T" denotes transposition in channel space. The Wronskian of two arbitrary solutions Φ_1 and Φ_2 is independent of r and equal to 0 because of the boundary condition $\Phi(0) = 0$. Demanding that

$$W(\Phi(r_\infty), \Phi_{\mathrm{as}}(r_\infty)) \equiv 0 , \tag{14}$$

we obtain for the partial-wave S matrix

$$S^J = - \left[\Phi'^T \frac{1}{\sqrt{mp}} H_1 - \Phi^T \sqrt{\frac{p}{m}} H_1' \right]^{-1} \left[\Phi'^T \frac{1}{\sqrt{mp}} H_2 - \Phi^T \sqrt{\frac{p}{m}} H_2' \right] , \tag{15}$$

where the prime on the Hankel functions denotes differentiation with respect to the argument pr. Since the matching is to Coulomb wave functions, what is actually obtained in this manner is the partial-wave S matrix with respect to the Coulomb force, denoted by S^C_{C+MM+N}. How to calculate the scattering amplitude is explained in Sec. V. The final step, the calculation of all the observables from the scattering amplitude, is standard [45–49]. See in particular Ref. [50] for the case of antinucleon-nucleon scattering.

III. THE SHORT-RANGE INTERACTION

The short-range dynamics is treated with the help of a boundary condition applied at a distance $r = b$. This boundary condition, called the P matrix, is the logarithmic derivative of the solution matrix $\Phi(r)$ at a distance $r = b$ from the origin

$$P = b \left(\frac{d\Phi}{dr} \Phi^{-1} \right)_{r=b} . \tag{16}$$

The factor b is included in this definition in order to make the P matrix dimensionless. The boundary-condition approach to strong interactions goes back to the work of Feshbach and Lomon [51] and earlier. The term P matrix was introduced by Jaffe and Low [52,53] for use with the bag model where at the energies of the eigenstates of the confined quark and gluon degrees of freedom the P matrix exhibits poles that are not necessarily also present in the S matrix. (For a review, see Ref. [54].) At this stage, we will not attempt to make any connection with multiquark states. In general, this boundary relates the inner- to the outer-region physics. In NN and $\overline{N}N$ scattering the short-range interaction is essentially unknown and has to be treated phenomenologically. The long-range physics one understands theoretically much better. The P-matrix formalism provides a useful separation between these two regions and has become a powerful tool in analyzing scattering data. In the Nijmegen partial-wave analyses of NN scattering data [5–7] the P-matrix method has already proven its power [55].

For the parametrization of the partial-wave P matrix, it is convenient to use a very simple model for the short-range dynamics. We assume that the interaction in each partial wave can be described by a spherical well, a potential which may depend on spin, isospin, and energy, but which is constant as a function of distance. The P matrix for such a potential can be evaluated analytically. For a single-channel spherical-well problem in a partial wave with orbital angular momentum ℓ it is given by

$$P_\ell = p'b \, J_\ell'(p'b) / J_\ell(p'b) , \tag{17}$$

where $J_\ell(\rho) = \rho j_\ell(\rho)$ with $j_\ell(\rho)$ the spherical Bessel function and $p'^2 = p^2 - 2mV$, V being the depth of the spherical-well potential. The prime on the Bessel function denotes differentiation with respect to the argument. In the case of $\overline{N}N$ scattering we take these short-range potentials to be complex in order to account for the annihilation into mesonic channels. The short-range interaction is in this manner described by a simple state-dependent optical potential [56]. It turns out that we can take the short-range spherical-well potential independent of the energy and still fit the data properly. This was not possible in the Nijmegen partial-wave analyses of the NN data: there we had to make the short-range potential energy dependent. That this is not necessary for $\overline{N}N$ scattering is probably because of the absence of high-quality data at low energies such as present in NN scattering. It is, however, crucial that we take the real parts to be dependent on spin and isospin. It also turned out that the imaginary parts of these short-range potentials could be taken independent of isospin. Each partial wave is thus parametrized by a maximum of three parameters, a complex spherical well for both isospin 0 and 1, where the imaginary parts are equal for both isospins. How many and which parameters are actually needed in each individual partial wave is discussed below in Sec. IX.

In the Nijmegen analyses of NN scattering data, a value of $b = 1.4$ fm for the boundary radius was found to be suitable. In the $\overline{N}N$ case, the results are rather sensitive on the choice of the value of b. The best results are obtained with $b = 1.3$ fm. Since we use in the outer region a real potential consisting of an electromagnetic and a meson-exchange part, the coupling to the mesonic channels is completely absorbed in the boundary condition. The radius b is therefore a clear measure for the range of the annihilation potential. The fact that the results are quite sensitive on b shows that this range is in fact approximately 1.3 fm. So we find definite indication that annihilation in $\overline{p}p$ scattering is a rather long-range process.

It remains to discuss the parametrization of the P matrix for the states with $\ell = J \pm 1$ coupled by the tensor force. In these cases it is convenient to use the method also employed in the NN case. For a certain value of the isospin, we start with a diagonal 2×2 P matrix and use additional parameters to describe the short-range mixing between the two coupled partial waves, as follows:

$$P = \begin{pmatrix} \cos\theta & \sin\theta \\ -\sin\theta & \cos\theta \end{pmatrix} \begin{pmatrix} P_1 & 0 \\ 0 & P_2 \end{pmatrix} \begin{pmatrix} \cos\theta & -\sin\theta \\ \sin\theta & \cos\theta \end{pmatrix} . \tag{18}$$

The mixing angle θ can, if necessary, be parametrized as a function of energy, but again in our analysis we can take it in all cases independent of the energy. We need these mixing angles only for the isospin $I = 0$ states, for the $I = 1$ states they can be set to zero.

Time-reversal invariance allows us to choose the phases of the physical states in such a way that the potential matrix is symmetric. The full S matrix, including all mesonic channels, is then also symmetric and of course unitary. When we restrict ourselves to the $\overline{N}N$ channels, then this sub-block of the S matrix is of course still symmetric, but no longer unitary. This reflects the disappearance of probability (flux) into the mesonic channels. Correspondingly, the P matrix in our case is still symmetric, but not Hermitian, as in NN scattering (below the pion-production threshold).

Why is the P-matrix approach to partial-wave analyses so convenient and powerful? One of the main reasons is that it allows an easy parametrization of the energy dependence of the scattering amplitudes. This can be seen as follows. The long-range interactions lead to rapid variations with energy of the amplitudes. These variations are much easier to parametrize when one uses the P matrix than the S matrix (or K matrix). For instance, in the presence of the Coulomb interaction, the S matrix has an essential singularity and a branchpoint at zero energy. However, if the Coulomb potential is included in the potential tail, these singularities and the corresponding left-hand cut are absent from the P matrix. Similarly, the left-hand cuts due to all meson exchanges included in the potential tail are absent from the P matrix. All these cuts, however, are present in the S matrix, in addition to the kinematical unitarity cut. The point is that the slow variations with energy of the amplitudes due to short-range interactions are easy to parametrize, once the rapid variations have been taken care of by explicitly including the corresponding long-range potentials in the Schrödinger equation. Of course, some left-hand cuts

remain, such as the cut due to uncorrelated two-pion exchange, as well as right-hand cuts due to the coupling to inelastic channels. These, however, lead to much slower energy variations of the amplitudes than the long-range electromagnetic interactions and one-pion exchange.

IV. THE POTENTIAL TAIL

In order to obtain a good description of the data, the long-range interaction between the particles, consisting of the electromagnetic interaction and the one-pion-exchange potential, must be included properly. These interactions are model independent in the sense that they are (or at least should be) the same in all models of the (anti)nucleon-nucleon force. The fit to the data is improved when realistic meson-exchange forces are used as intermediate-range potential.

The long-range electromagnetic potential is included to order $\alpha = e^2/4\pi$, the fine-structure constant. The one-photon-exchange potential is derived from the phenomenological electromagnetic Lagrangian

$$\mathcal{L}_\gamma = e\, Q\, [i\overline{\psi}\gamma_\mu\psi]\, A^\mu \;+\; e\, \frac{\kappa}{4M}\, [\overline{\psi}\sigma_{\mu\nu}\psi]\, (\partial^\mu A^\nu - \partial^\nu A^\mu)\ ,$$

$$(19)$$

where Q is the nucleon charge in units of $e > 0$ and κ is the anomalous magnetic moment, for proton and neutron $\mu_p = 1 + \kappa_p = 2.793$, and $\mu_n = \kappa_n = -1.913$, respectively. ψ is the proton or neutron field and A^μ the photon field. If the spatial extension of the nucleons is taken into account, the charge and magnetic moments are in momentum space replaced by the Dirac form factor $F_1(t)$ and the Pauli form factor $F_2(t)$, which are functions of the four-momentum transfer t. The static limits $t = 0$ are

$$F_1^p(0) = 1 \ , \quad F_1^n(0) = 0 \ , \quad F_2^p(0) = \frac{\kappa_p}{2M_p} \ , \quad F_2^n(0) = \frac{\kappa_n}{2M_n} \ . \tag{20}$$

In the point-particle approximation the momentum dependence of these form factors, reflecting the inner structure of the nucleons, is neglected. In this approximation we end up with the spin-dependent one-photon-exchange potentials for $r > b$

$$V_\gamma(r) \;=\; -\frac{\alpha'}{r} + \frac{\mu_p^2}{4M_p^2}\,\frac{\alpha}{r^3}\, S_{12} + \frac{8\mu_p - 2}{4M_p^2}\,\frac{\alpha}{r^3}\,\mathbf{L}\cdot\mathbf{S} \quad \text{for } \overline{p}p \to \overline{p}p\ , \tag{21}$$

and

$$V_\gamma(r) \;=\; \frac{\mu_n^2}{4M_n^2}\,\frac{\alpha}{r^3}\, S_{12} \quad \text{for } \overline{n}n \to \overline{n}n\ . \tag{22}$$

These potentials are obtained by calculating the one-photon-exchange diagrams in momentum space and applying a Fourier transformation to configuration space. The momentum dependence of the form factors can be taken into account. This leads to short-range modifications of the one-photon-exchange potential. Since we use

only the potential outside $r = b = 1.3$ fm, we did not include these effects. The use of α' in the central potential for $\overline{p}p \to \overline{p}p$ takes care of the main relativistic corrections to the Coulomb potential [57,58]. It is given by

$$\alpha' \;=\; \alpha\, 2p/(M v_{\text{lab}})\ , \tag{23}$$

where v_{lab} is the velocity of the antiproton in the laboratory system. In order to appreciate the order of magnitude of this factor, at 600 MeV/c for instance, where $v_{\text{lab}} = 0.54$, one has $\alpha' = 1.135\alpha$. The spin-orbit poten-

tial comes from the interaction of the magnetic moment of one particle with the Coulomb field of the other particle (and is consequently absent in $\bar{n}n \to \bar{n}n$). It includes a relativistic correction due to the Thomas precession. The tensor potential comes from the interaction of the two magnetic moments. In our energy range the Coulomb and the magnetic-moment interaction are the dominant

electromagnetic effects. The vacuum-polarization potential [59], which is important [5] in low-energy pp scattering (below $T_{\text{lab}} = 30$ MeV), has a negligible influence here. Two-photon-exchange effects [58] are neglected as well.

The following simple one-pion-exchange potential without a form factor is used:

$$V_\pi(r) = f^2_{NN\pi} \frac{M}{\sqrt{p^2 + M^2}} \frac{m^2}{m^2_{\pi\pm}} \frac{1}{3} \left[\sigma_1 \cdot \sigma_2 + S_{12} \left(1 + \frac{3}{mr} + \frac{3}{(mr)^2} \right) \right] \frac{e^{-mr}}{r} . \tag{24}$$

The mass difference between the neutral π^0 and charged $\pi^\pm$ pion is included, so we take $m = m_{\pi^0}$ for the elastic reactions $\bar{p}p \to \bar{p}p$ and $\bar{n}n \to \bar{n}n$, and $m = m_{\pi\pm}$ for the off-diagonal charge-exchange transitions $\bar{p}p \leftrightarrow \bar{n}n$. In principle, the pion-nucleon coupling constant is charge dependent due to the mass difference between the up and down quarks and due to the electromagnetic corrections. We introduce here the relevant coupling constants $f^2_{NN\pi}$ at the different vertices

$$f^2_p \equiv f^2_{pp\pi^0} \, , \quad f^2_n \equiv f^2_{nn\pi^0} \, , \quad 2f^2_c \equiv f_{pn\pi^+}f_{np\pi^-} \, , \tag{25}$$

for the reactions $\bar{p}p \to \bar{p}p$, $\bar{n}n \to \bar{n}n$, and $\bar{p}p \leftrightarrow \bar{n}n$, respectively. In the PWA a charge-independent pion-nucleon coupling constant is used, where $f^2_p = f^2_n = f^2_c = 0.0745$, taken from the most recent Nijmegen pp PWA [60]. In Sec. IX, however, this assumption is relaxed when we determine the charged-pion coupling constant from the charge-exchange data by adding f^2_c as a free parameter.

To improve the description of the data, some sort of heavy-meson-exchange potential has to be added to one-pion exchange in the outer region. Since the tails of realistic NN potentials are remarkably similar, it probably does not matter very much which potential one picks, provided it gives a good description of the NN scattering data. We have opted for the charge-conjugation-transformed version of the Nijmegen one-boson-exchange

soft-core NN potential [30], which is one of the best NN potentials available. (The use of C conjugation rather than G conjugation is more natural when one works on the physical particle basis.) The tail of this potential has already been used in the Nijmegen pp and np partial-wave analyses, and the tail of the corresponding Nijmegen soft-core hyperon-nucleon potential [61,62] has been used by us in our PWA of the reaction $\bar{p}p \to \bar{\Lambda}\Lambda$ [31,32]. The following heavy-boson-exchange potentials are included.

(1) Pseudoscalar-meson exchange. Included are $\eta(549)$ and $\eta'(958)$ exchange. For the pseudoscalars, including the pion, we use the pseudovector type of Lagrangian:

$$\mathcal{L}_{\text{PV}} = \sqrt{4\pi} \frac{f}{m_{\pi\pm}} \left[i\bar{\psi}\gamma_\mu\gamma_5\psi \right] \partial^\mu \Phi_P . \tag{26}$$

Although equivalent to the pseudoscalar type of interaction for one-meson exchange between protons, the pseudovector interaction is favored because it gives a more reasonable two-pion-exchange potential and because it leads to at most small breakings of flavor symmetry for the coupling constants of the pseudoscalar nonet to baryons [31]. The scaling mass $m_{\pi\pm}$ is conventionally introduced to make the coupling constant f dimensionless.

(2) Vector-meson exchange. Included are $\rho(770)$, $\omega(782)$, and $\phi(1019)$ exchange. The Lagrangian (in terms of rationalized coupling constants) is

$$\mathcal{L}_V = \sqrt{4\pi}g \left[i\bar{\psi}\gamma_\mu\psi \right] \Phi^\mu_V + \sqrt{4\pi}\frac{f}{4M_p} \left[\bar{\psi}\sigma_{\mu\nu}\psi \right] (\partial^\mu\Phi^\nu_V - \partial^\nu\Phi^\mu_V) . \tag{27}$$

(3) Scalar-meson exchange. We include $a_0(783)$, $f_0(975)$, and $f'_0(760)$ exchange. The Lagrangian is

$$\mathcal{L}_S = \sqrt{4\pi}g \left[\bar{\psi}\psi \right] \Phi_S . \tag{28}$$

The scalar mesons have always been a controversial topic. In early one-boson-exchange models for the NN interaction there was a clear need for an isoscalar scalar "σ" meson with an effective mass of about 550 MeV [63–65]. While no such low-mass particle exists, there was some evidence in production experiments for a broad structure $\varepsilon(760)$ under the ρ^0, often explained away as a strong $\pi\pi$ final-state interaction. Later it was pointed out [66,67,43]

that such a wide ($\Gamma \approx 640$ MeV) $\varepsilon(760)$ simulates the narrow-"σ" exchange in one-boson-exchange models for the NN interaction.

The situation in phase-shift analyses of $\pi\pi$ scattering data, obtained from reactions as $\pi N \to \pi\pi N$, has for a long time been confusing and not conclusive [68]. In these analyses the assumption has always been that only π exchange is relevant, while a_1 exchange can be neglected. Very recently, however, the situation has been clarified [69]. Data on $\pi N \uparrow \to \pi^+\pi^- N$ using a polarized target provide unambiguous evidence for a broad $I = 0$ $0^{++}(750)$ state, when a proper amplitude analysis is done, including also a_1 exchange. In a similar ampli-

tude analysis of data on $K^+ n \uparrow \to K^+ \pi^- p$ [70] evidence is found for $I = 1/2\ 0^+(887)$ strange scalar mesons under the $K^*(892)$.

In the quark model, several mechanisms give rise to scalar ($J^P = 0^+$) mesons. The simplest model is the $^3P_0\ \overline{Q}Q$ states. Then there are the glueball states and the cryptoexotic $\overline{Q}^2 Q^2$ states [71]. A physical scalar meson will in general be a mixture of $\overline{Q}Q$, $\overline{Q}^2 Q^2$, and glueball components. The $\overline{Q}Q$ states are expected [72] near the other $^3P\ \overline{Q}Q$ mesons, that is around 1250 MeV. Glueballs are also not very likely to exist below 1000 MeV [73]. For the $\overline{Q}^2 Q^2$ states, however, one [71] does predict a low-lying nonet of scalar mesons. The lowest state, with only nonstrange quarks, has $I = 0$ and decays into $\pi\pi$. It can be identified with the $\varepsilon(760)$ under the ρ^0. This nonet contains also a nearly degenerate set of $I = 0$ and $I = 1$ cryptoexotic scalar mesons [like the $\rho(770)$ and $\omega(782)$] with an $\bar{s}s$ pair. These are easily identified as the $f_0(975)$ and $a_0(983)$ mesons, previously called $S^*(975)$ and $\delta(983)$, respectively, with their relatively large branching ratios into $\overline{K}K$. The nonet is completed by a set of broad $I = 1/2$ strange mesons $K_0^*(887)$ seen [74] under the $K^*(892)$.

(4) Next to these conventional mesons, the Nijmegen soft-core potential (originally derived from Regge-pole theory) also contains pomeron exchange, which in QCD is understood as color-singlet two-gluon or multigluon exchange [75–77], and the weak diffractive scalarlike part of the tensor-meson exchanges. The short-range nonlocal terms of the potential are neglected, which is a very good approximation outside $r = b = 1.3$ fm.

The consequences of meson exchanges for the $\overline{N}N$ interaction have been examined by many authors, for instance by Dover and Richard [78–80]. It turns out from a qualitative investigation that while in the NN case there is a strong coherence between the isospin $I = 1$ spin-orbit forces, in the $\overline{N}N$ case very strong tensor forces occur, especially for isospin $I = 0$. In the NN system the vector $\omega(782)$ and the scalar $f_0'(760)$ exchange make up the strong spin-orbit force that splits the $^3P_{0,1,2}$ phase shifts, but the central potentials of these exchanges largely cancel each other. Similarly, the spin-orbit forces due to the exchange of the vector $\rho(770)$ and the scalar $a_0(983)$ add up, but the central potentials cancel. Applying charge conjugation to the different meson exchanges, one sees that in the $\overline{N}N$ potential the central potentials from $\omega(782)$ and $f_0'(760)$ exchange add coherently to a very strong attractive potential. This has led to speculation about the existence of $\overline{N}N$ bound states and resonances [81–85]. The tensor potentials from $\rho(770)$ and $\pi(140)$ exchange also add up and dominate the charge-exchange reaction $\bar{p}p \to \bar{n}n$. The same phenomenon is present in the reaction $\bar{p}p \to \overline{\Lambda}\Lambda$, where $K(494)$ and $K^*(892)$ exchange conspire to build up the strong tensor force that is the hallmark of this reaction [31].

V. THE AMPLITUDES

The evaluation of the scattering amplitude in the presence of electromagnetic effects is a nontrivial problem that requires special care. In the pp PWA the precise values and energy dependence of the phase shifts are influenced significantly by the electromagnetic interaction. The same will obviously also be true in the $\bar{p}p$ case.

We start by discussing the case where next to the nuclear force we only have the Coulomb potential to deal with. The scattering amplitude due to the Coulomb force is given by

$$
\begin{aligned}
\langle s'm'a'|M_C(\theta)|s\,m\,a\rangle &= -\delta_{ss'}\delta_{mm'}\delta_{aa'}\,\frac{\eta_a}{p_a(1-\cos\theta)}e^{-i\eta_a\ln\frac{1}{2}(1-\cos\theta)+2i\sigma_{0,a}} \\
&= -\delta_{ss'}\delta_{mm'}\delta_{aa'}\,\frac{\eta_a}{2p_a}\frac{e^{2i\sigma_{0,a}}}{(\sin^2\frac{1}{2}\theta)^{1+i\eta_a}}\ .
\end{aligned}
\tag{29}
$$

The partial-wave decomposition of $M_C(\theta)$ in terms of Coulomb phase shifts and Legendre polynomials does not converge pointlike, due to the infinite range of the Coulomb potential. However, it can be summed in the sense of distributions [86–88] to give the Coulomb amplitude Eq. (29). In order to make a partial-wave decomposition of the scattering amplitude, the total scattering amplitude $M_{C+N}(\theta)$ is split as follows:

$$
M_{C+N}(\theta) = M_C(\theta) + M_{C+N}^C(\theta)\ ,
\tag{30}
$$

where the amplitude $M_{C+N}^C(\theta)$ is the nuclear scattering amplitude in the presence of the Coulomb potential. Its partial-wave decomposition reads

$$
\begin{aligned}
\langle s'm'a'|M_{C+N}^C(\theta)|s\,m\,a\rangle &= \sum_{\ell\ell'J}\sqrt{4\pi(2\ell+1)}\,i^{\ell-\ell'}\,C_{0\ \ m\ m}^{\ell\ s\ J}\,C_{m-m'\ m'\ m}^{\ell'\ \ s'\ J}\,Y_{m-m'}^{\ell'}(\theta) \\
&\quad \times\langle\ell's'a'|S_C^{1/2}(S_{C+N}^C-1)S_C^{1/2}|\ell\,s\,a\rangle/2ip_a\ ,
\end{aligned}
\tag{31}
$$

where S_{C+N}^C is the nuclear S matrix in the presence of the Coulomb force. The total S matrix S_{C+N}, due to the Coulomb and nuclear interaction, is then given by

$$
S_{C+N} = S_C^{1/2}\,S_{C+N}^C\,S_C^{1/2}\ .
\tag{32}
$$

S_C is the Coulomb S matrix with matrix elements

$$
\langle\ell's'a'|S_C|\ell\,s\,a\rangle = \delta_{\ell\ell'}\delta_{ss'}\delta_{aa'}\,\exp(2i\sigma_{\ell,a})\ .
\tag{33}
$$

The nuclear S matrix in the presence of the Coulomb

force S^C_{C+N} is obtained by solving the Schrödinger equation numerically and matching to Coulomb wave functions (see Sec. II). It is given by Eq. (15).

Next we discuss the generalization to the case where next to the Coulomb force also the magnetic-moment interaction is present [89]. Although this latter potential has a finite range and consequently the partial-wave

decomposition converges, it is still much more practical to split off in the scattering amplitude the contribution of the magnetic-moment interaction. In this way the magnetic-moment interaction can be included in all partial waves and the summation in the nuclear amplitude converges much faster. We thus write

$$M_{C+\text{MM}+N}(\theta) = M_C(\theta) + M^C_{C+\text{MM}}(\theta) + M^{C+\text{MM}}_{C+\text{MM}+N}(\theta) . \tag{34}$$

Here $M^C_{C+\text{MM}}(\theta)$ is the scattering amplitude of the magnetic-moment interaction in the presence of the Coulomb force. Since this amplitude is almost exactly in phase with the Coulomb scattering amplitude $M_C(\theta)$, it is essential that the effect of the magnetic-moment interaction is evaluated in Coulomb-distorted-wave Born approximation (CDWBA), and not in plane-wave Born approximation, as was pointed out by Knutson and Chiang [90]. The contribution, in CDWBA, of the magnetic-moment interaction to the K matrix is

$$\langle \ell' s' a' | K_{\text{MM}} | \ell \, s \, a \rangle = -\delta_{aa'} \frac{M_a}{p_a} \int_0^\infty dr \, F_{\ell'}(\eta_{a'}, p_{a'} r) V_{\text{MM}}(r) F_\ell(\eta_a, p_a r) . \tag{35}$$

Integrals of this type can be evaluated very rapidly and accurately by a backward-recursion algorithm [91]. The magnetic-moment interaction V_{MM} is given in Eq. (21) for $\bar{p}p \to \bar{p}p$ and in Eq. (22) for $\bar{n}n \to \bar{n}n$. All these partial-wave contributions are subsequently summed to obtain the total amplitude $M^C_{C+\text{MM}}(\theta)$. In practice it turns out that the spin-orbit potential of the magnetic-moment interaction leads to a contribution Z_{LS} to $\langle 11a | M^C_{C+N}(\theta) | 10a \rangle$ that converges much too slowly to be summed term by term. This part can be summed analytically [90]. For antiproton-proton scattering the result is

$$Z_{LS} = -\frac{M_p f_{LS}}{\sin\theta\sqrt{2}} \left(e^{-i\eta \ln \frac{1}{2}(1-\cos\theta)} - \frac{1}{2}(1 - \cos\theta) \right) , \tag{36}$$

where we have defined

$$f_{LS} = -\frac{\alpha}{4M_p^2}(8\mu_p - 2) . \tag{37}$$

There is a similar contribution $-Z_{LS}$ to $\langle 10a | M^C_{C+N}(\theta) | 11a \rangle$. The corresponding result for pp scattering [90] is the properly symmetrized version of this expression. The partial-wave decomposition of $M^{C+\text{MM}}_{C+\text{MM}+N}(\theta)$, the nuclear scattering amplitude in the presence of the Coulomb force and the magnetic-moment interaction, is similar to Eq. (31), but there now appears the following S matrix:

$$S_{C+\text{MM}+N} = S_C^{1/2} \left(S^C_{C+\text{MM}} \right)^{1/2} S^{C+\text{MM}}_{C+\text{MM}+N} \left(S^C_{C+\text{MM}} \right)^{1/2} S_C^{1/2} . \tag{38}$$

Since the magnetic-moment interaction contains a tensor part, the matrix $S^C_{C+\text{MM}}$ is not diagonal in orbital angular momentum. However, the square root of this matrix is still well defined. What it all comes down to is to rewrite the S matrix in the following manner in order to split off the Coulomb amplitude M_C and the amplitude $M^C_{C+\text{MM}}$ due to the magnetic-moment interaction in the presence of the Coulomb force

$$S_{C+\text{MM}+N} - 1 = (S_C - 1) + S_C^{1/2} \left(S^C_{C+\text{MM}} - 1 \right) S_C^{1/2} + S_C^{1/2} \left(S^C_{C+\text{MM}} \right)^{1/2} \left(S^{C+\text{MM}}_{C+\text{MM}+N} - 1 \right) \left(S^C_{C+\text{MM}} \right)^{1/2} S_C^{1/2} . \tag{39}$$

Other electromagnetic effects, like vacuum polarization, can be treated in a similar way. For a more extensive discussion we refer to Ref. [89]. Because of the long range of the magnetic-moment interaction the matrix elements of $S^{C+\text{MM}}_{C+\text{MM}+N}$ are hard to calculate. We will use the approximation

$$S^{C+\text{MM}}_{C+\text{MM}+N} \approx S^C_{C+N} . \tag{40}$$

Exactly the same approximation is made in the Nijmegen NN partial-wave analyses [89].

VI. THE PHASE SHIFTS

In this section we give the parametrization of the $\overline{N}N$ S matrix in terms of phase-shift and inelasticity parameters. We first seek guidance in the way this is done in analyses of NN scattering below the pion-production threshold where the S matrix is unitary and symmetric. The symmetry of the S matrix is a consequence of time-reversal invariance which allows one to choose the phases of the in and out states such that the coupled-channels

potential matrix, and thus the S matrix, is symmetric. If there is conservation of flux, the S matrix is unitary.

The phase shift for uncoupled partial waves with $\ell = J$, $s = 0, 1$ is defined by parametrizing the 1×1 S matrix as

$$S^J = \exp(2i\delta) . \tag{41}$$

One usually denotes the different phase shifts by δ_ℓ for singlet $s = 0$ waves, and by $\delta_{\ell,J}$ for triplet $s = 1$ waves. For the partial waves with $\ell = J \pm 1$, $s = 1$ coupled by a tensor force one writes the 2×2 S matrix in terms of two phase shifts $\delta_{J-1,J}$, $\delta_{J+1,J}$ and one mixing parameter ε_J. A popular parametrization is the "eigenphase" convention of Blatt and Biedenharn [92], in which the symmetric S matrix is diagonalized by way of a rotation

$$S^J = \exp(-i\varepsilon_J\sigma_y) \exp(2i\delta) \exp(i\varepsilon_J\sigma_y) , \tag{42}$$

where

$$\delta = \begin{pmatrix} \delta_{J-1,J} & 0 \\ 0 & \delta_{J+1,J} \end{pmatrix} . \tag{43}$$

More often one uses the "bar-phase" convention of Stapp, Ypsilantis, and Metropolis [93], in which

$$S^J = \exp(i\bar{\delta}) \exp(2i\bar{\varepsilon}_J\sigma_x) \exp(i\bar{\delta}) . \tag{44}$$

An advantage of the "bar-phase" convention is that the parameters go to zero when the interaction vanishes, unlike the mixing parameter in the "eigenphase" convention. Only in the former case is the mixing parameter a measure of the strength of the off-diagonal tensor force. We will use the "bar-phase" parametrization for the three elastic parameters, since this is at present the common choice in analyses of NN scattering.

In the presence of coupling to annihilation channels the S matrix describing $\overline{N}N$ scattering is only a submatrix of the much larger coupled-channels S matrix, and is therefore still symmetric, but no longer unitary. This doubles the number of parameters needed. The parametrization of the S matrix for uncoupled partial waves with $\ell = J$, $s = 0, 1$ in the presence of annihilation requires two parameters. One writes

$$S^J = \eta \exp(2i\delta) , \tag{45}$$

with $|\eta| \leq 1$. To denote the inelasticities for the different partial waves we will use a similar notation as for the phase shifts: η_ℓ for singlet $s = 0$ waves, and $\eta_{\ell,J}$ for triplet $s = 1$ waves. For the coupled partial waves with $\ell = J \pm 1$, $s = 1$ six parameters are needed, and it is not so easy to think of a convenient parametrization which satisfies all constraints from unitarity, is completely general, and free from nontrivial ambiguities. Fortunately, the essential work has already been done by Bryan [94] and others [95–97] in the case of NN scattering above the pion-production channel. Bryan generalizes the "bar-phase" convention by writing

$$S^J = \exp(i\bar{\delta}) \exp(i\bar{\varepsilon}_J\sigma_x) H^J \exp(i\bar{\varepsilon}_J\sigma_x) \exp(i\bar{\delta}) , \tag{46}$$

where H is a three-parameter real and symmetric matrix representing inelasticity. Bryan calls this matrix N, but we use H (capital η) to stress the analogy with the case of uncoupled partial waves written in the form

$$S^J = \exp(i\bar{\delta})\, \eta \, \exp(i\bar{\delta}) . \tag{47}$$

If the inelasticity vanishes, then H tends to the unit matrix, and the "bar-phase" parametrization is recovered. There are several nice ways to parametrize H, but we find it convenient to follow Klarsfeld [96], who diagonalizes H in Blatt-Biedenharn fashion

$$H^J = \exp(-i\omega_J\sigma_y) \begin{pmatrix} \eta_{J-1,J} & 0 \\ 0 & \eta_{J+1,J} \end{pmatrix} \exp(i\omega_J\sigma_y) , \tag{48}$$

where the diagonal matrix contains the "eigeninelasticities" $\eta_{J-1,J}$ and $\eta_{J+1,J}$. In this way the partial-wave annihilation cross section depends only on the "eigeninelasticities," since it is proportional to

$$\mathrm{Tr}\,(1 - H^2) = 2 - \eta_{J-1,J}^2 - \eta_{J+1,J}^2 . \tag{49}$$

If the phase parameters are actually searched for on a computer, it is better to write all inelasticities as $\eta = \cos 2\rho$. In this way, all parameters are real and unbounded. The mixing parameter ω_J is finite as the inelasticity vanishes, just as the mixing parameter ε_J in the "eigenphase" convention tends to a finite value when the off-diagonal tensor force goes to zero. Sprung [97] has extended the Bryan parametrization to allow the use of "eigenphases." In this case one writes

$$S^J = \exp(-i\varepsilon_J\sigma_y) \exp(i\delta) H^J \exp(i\delta) \exp(i\varepsilon_J\sigma_y) . \tag{50}$$

The matrix H in that case is, in general, not equal to the matrix H in Eq. (46). As stated above, we will use the "bar phases." The algorithm, due to Bryan [94], to extract the phase parameters and inelasticities from the S matrix presented in numerical form is reviewed in the Appendix.

VII. STATISTICS

Statistics is an essential ingredient in analyses of large amounts of scattering data. The theoretical predictions are compared with the experimental data using a least-squares-fitting procedure in which the model parameters are adjusted to the data. During this process one continually scrutinizes the data and passes sentence on the quality of different sets, which sometimes have to be rejected on the basis of statistical criteria. This goes on until a final verdict is reached and the building of the data set is completed. In this section this procedure is outlined and the statistical tools required for our purpose are presented. A more exhaustive treatment can be found in Ref. [5].

We start by assuming for the moment that the mea-

surements have no normalization uncertainties and that no other type of systematic error is present. In a certain experiment, denoted by a subscript a, one has measured N_a data points. Each such measurement with statistical error is denoted by $E_{a,i} \pm \varepsilon_{a,i}$ $(i = 1, \ldots, N_a)$. The model prediction for a certain data point is given as $M_{a,i}(\mathbf{p})$, where the model parameters are arranged in a vector $\mathbf{p}$, with entries p_α $(\alpha = 1, \ldots, N_{\text{par}})$. The parameters are adjusted to the data by minimizing the χ^2 function

$$\chi^2(\mathbf{p}) = \sum_a \chi_a^2(\mathbf{p}) = \sum_a \sum_{i=1}^{N_a} \left[\frac{M_{a,i}(\mathbf{p}) - E_{a,i}}{\varepsilon_{a,i}} \right]^2 \quad (51)$$

with respect to all parameters.

In practice, however, measurements usually do have an overall normalization uncertainty, specified by the experimentalists. These errors can be taken care of by introducing for each group of data a normalization parameter ν_a with error $\varepsilon_{a,0}$. The normalization of a certain group is then given as $\nu_a = 1 \pm \varepsilon_{a,0}$. This means essentially that for each group with a finite normalization uncertainty another free parameter ν_a has been introduced, to be determined in the fit, as well as an additional datum 1 with error $\varepsilon_{a,0}$. Since we want to restrict the parameter space to the model parameters only, we employ the following trick to take the normalization parameters into account. We redefine the χ^2 function as follows:

$$\chi^2(\mathbf{p}) = \sum_a \chi_a^2(\mathbf{p}) = \sum_a \min \sum_{i=1}^{N_a} \left[\frac{\nu_a M_{a,i}(\mathbf{p}) - E_{a,i}}{\varepsilon_{a,i}} \right]^2 + \left[\frac{\nu_a - 1}{\varepsilon_{a,0}} \right]^2 . \quad (52)$$

In this way, the normalizations are adjusted trivially, by minimizing in each iteration a quadratic function. In case the normalization of an experiment is completely unknown, $\varepsilon_{a,0} = \infty$ and we can remove the second term on the right-hand side of Eq. (52). The corresponding normalization ν_a is determined in the fit. We say the normalization is "floated." If the normalization is exactly known, we fix the normalization at $\nu_a = 1$ and we can remove again the second term. Angle-dependent normalization errors can be treated in a similar manner. The minimum value $\chi_{\min}^2 = \chi^2(\mathbf{p})|_{\mathbf{p}=\mathbf{p}_{\min}}$ is reached when

$$\partial \chi^2(\mathbf{p})/\partial p_\alpha \equiv 0 , \quad (53)$$

for all values of α. At this point one defines the error matrix E of the parameters as

$$(E^{-1})_{\alpha\beta} = \frac{1}{2} \partial^2 \chi^2(\mathbf{p})/\partial p_\alpha \partial p_\beta |_{\mathbf{p}=\mathbf{p}_{\min}} . \quad (54)$$

The standard error on the parameter p_α is $(E_{\alpha\alpha})^{1/2}$. Assuming that the χ^2 function is quadratic near its minimum, one can show that this is the variation in p_α that gives a rise $\Delta\chi^2 = 1$ in $\chi_{\min}^2$, when the remaining parameters are refitted [98].

According to this discussion the following integers can be defined. In the fit one must determine N_n normalization parameters as well as N_{par} model parameters. The actual number of free parameters is therefore $N_{\text{fp}} = N_{\text{par}} + N_n$. Of these N_n normalization parameters N_{ne} have a finite normalization error and the rest $N_{\text{nf}} = N_n - N_{\text{ne}}$ is the number of "floated" normalizations. The total number of experimental scattering observables is N_{obs} and the actual number of scattering data is $N_{\text{data}} = N_{\text{obs}} + N_{\text{ne}}$. The number of degrees of freedom is $N_{\text{df}} = N_{\text{data}} - N_{\text{fp}} = N_{\text{obs}} - N_{\text{par}} - N_{\text{nf}}$.

In the process of screening the database, we employ certain rejection criteria to remove data points that spoil the statistical quality of the data set, for instance by un-

derestimated statistical errors or by unspecified systematic errors. When statistical errors are underestimated, data pretend to give more information than they actually do, causing false results. By systematic errors we mean those errors that do not average to zero when the measurement is repeated many times, causing them to have a correlated effect on the data. When not treated correctly, systematic errors can bias the values of the model parameters and therefore also of the phase parameter. A detailed discussion of this point can again be found in Ref. [5]. Of course, we only reject data if there is conclusive evidence against them. The rejection criteria are constructed in such a way that in a purely statistical ensemble they have a very small chance to occur. The following rejection criteria have been employed by us.

(i) An individual data point $E_{a,i}$ that has $\chi_{a,i}^2 > 9$ is rejected. Rejection of such outliers will give more accurate values for the model parameters. This rejection criterium corresponds to the usual three-standard-deviation rule. It implies that a correct datum has at most a chance of 0.27% to be rejected. The same criterium applies to an experimental normalization. If it contributes more than 9 to $\chi_{\min}^2$, this datum is rejected and the normalization is floated.

(ii) A group of N_a data is rejected if its χ_a^2 in the multienergy fit is less than a minimum $\chi_{\text{low}}^2(N_a)$. The values for χ_{low}^2 can be found in Ref. [5]. They are constructed such that again the chance for a correct group to be rejected is at most 0.27%. This rejection criterium is used as a means to avoid systematic errors. Very low values of χ^2 are very probably caused by systematic errors present in the data and are *not* a virtue of a model. This criterium generally does not seem to be appreciated by the uninitiated in statistical methods.

(iii) A group of N_a data is also rejected if its χ_a^2 in the multienergy fit exceeds a maximum $\beta\chi_{\text{high}}^2(N_a)$, where $\beta = N_{\text{df}}/(N_{\text{df}} + N_{\text{par}})$. The values for χ_{high}^2 can also be found in Ref. [5].

VIII. THE NIJMEGEN 1993 ANTIPROTON-PROTON DATABASE

A. Set-up of the 1993 database

In order to perform a $\bar{p}p$ PWA, we first had to put together a statistically sound data set. In NN analyses, one has over 30 years experience with the data, and by now a proper database is more or less agreed upon. In the $\bar{p}p$ case, we must start from scratch, but fortunately we can use the experience of the NN analyses to arrive at an acceptable $\bar{p}p$ database. Let us summarize the general features of our database. We will include in our $\bar{p}p$ database all available $\bar{p}p$ scattering data below antiproton laboratory momentum $p_{\text{lab}} = 925$ MeV/c published in a regular physics journal since 1968. We do not take into account data published only in conference abstracts, in conference proceedings, and/or theses. The reason we restrict ourselves to this momentum range is that it corresponds roughly to the energy range of the NN partial-wave analyses below kinetic energy $T_{\text{lab}} = 350$ MeV (momentum 925 MeV/c corresponds to $T_{\text{lab}} = 379$ MeV) and that we want to include the accurate backward elastic cross sections between 406 and 922 MeV/c taken by Alston-Garnjost [117]. Low-energy data, below $p_{\text{lab}} = 175$ MeV/c, so $T_{\text{lab}} \approx 15$ MeV, are of course almost nonexistent here. Only scattering observables are analyzed, other "data" like for instance the real-to-imaginary ratio of the forward scattering amplitude or the slope of the $\bar{p}p$ forward nuclear amplitude are omitted, since the extraction of these quantities from the data is model dependent. A summary of the Nijmegen 1993 $\bar{p}p$ database can be found in Table I.

Several experiments [133–135] have reported a resonant structure in the antiproton-proton total cross section near 490 MeV/c without agreeing, however, on the exact position, strength, and width of a possible resonance. We do not include these data in the PWA, since more recent and accurate measurements of total cross sections [136,111,109,137,114] have convincingly ruled out the existence of this type of rather broad resonance. (A more narrow type of resonance, however, is not ruled out by the existing data. In fact, there is some statistical evidence for a narrow structure in backward elastic cross sections around 509 MeV/c [138]. Probably, only an accurate measurement of the backward charge-exchange cross section can definitely settle this issue.)

High-quality total cross sections below 400 MeV/c have been measured at LEAR by the PS172 Collaboration [106]. The effects of the pure Coulomb force and Coulomb-nuclear interference are not significant, except perhaps at low momenta $\lesssim 300$ MeV/c. This may be the reason why we had to reject the data at the two lowest momenta.

In a number of experiments [134,139,111,140–144] the $\bar{p}p$ annihilation cross section into charged mesons has been measured. We cannot include these data, not even with a floated normalization, since the momentum dependence of the cross section for annihilation into neutral mesons is not known. At LEAR the total annihilation cross section, including annihilation into neutral chan-

nels, has been measured from 180 to 600 MeV/c by the PS173 group [105,100]. These last data are included.

We do not include integrated elastic-cross-section data [110,104,145,113,115], due to difficulties in a proper treatment of Coulomb and Coulomb-nuclear interference. Integrated charge-exchange cross sections, on the other hand, are included in the database. In two experiments [108,99] this observable was measured over a large momentum region. For the experiment of Ref. [99] data points at the lowest momenta are rejected since they are in conflict with more recent measurements done at LEAR by the PS173 group [103]. Our PWA clearly favors this last experiment.

In the pre-LEAR era a very large part of the experimental data on $\bar{p}p$ scattering consisted of elastic differential cross sections [110,104,129,132,128,113]. The most accurate data were those taken by Eisenhandler *et al.* at 690, 790, and 860 MeV/c (and higher momenta) [128]. With the exception of the data at 194.8 MeV/c of Ref. [104] and the data at 910 MeV/c of Ref. [132] we find these pre-LEAR data to be consistent. An accurate measurement of the backward elastic differential cross section at $\cos\theta = -0.994$ was done by Alston-Garnjost *et al.* [117] between 406 and 922 MeV/c. Since 1983, differential cross sections on $\bar{p}p \to \bar{p}p$ have been measured by different groups at LEAR and at KEK. For an extensive discussion of these data we refer to the next subsection.

A number of pre-LEAR experiments determined the elastic differential cross section at forward scattering angles in order to study the Coulomb-nuclear-interference region [146,118,112,147]. At LEAR this was done by the collaborations PS172 [107,125] and PS173 [148,149]. In general, all these data are well described in the PWA, although in some cases data points in the extreme-forward region had to be rejected since they are contaminated by multiple Coulomb scattering in the target (so-called Molière scattering).

Some of the most important results coming from LEAR are the high-quality elastic analyzing-power A_y (polarization) data, measured by the PS172 [122,123] and PS198 [130,120] collaborations at a number of energies above 439 MeV/c. Since in the pre-LEAR era only very few and inaccurate data points existed [132,127,131], these experiments mean real progress. We find the data of PS172 and PS198 to be consistent, except for their normalizations. In our PWA we float the normalizations of the A_y data at 497, 523, and 679 MeV/c. PS172 has also obtained the first (not very accurate) results on the elastic D_{yy} depolarization [150]. For these data we do not take a normalization error into account, in view of the large error bars.

Before the advent of LEAR in 1983, also charge-exchange differential observables were scarce. Some differential cross sections existed [119,129,151,121,152], but these were not very accurate. Since 1984, however, the situation has improved enormously. High-quality differential cross sections have been obtained at KEK between 392 and 781 MeV/c [116], and at LEAR by the PS173 group at low momenta between 183 and 590 MeV/c [103]. One of the most important experiments at LEAR has

TABLE I. Reference table of antiproton-proton scattering data below 925 MeV/c.

p_{lab} (MeV/c)	No.[a] type[b]	χ^2_{min}	Norm error	Pred. norm[c]	Rejected[d]	Ref.	Comm.
119.0– –923.0	50 σ_{ce}	29.2	3–5%	1.098	$\leq$385.0, #=8	[99]	k, m
176.8– –396.1	5 σ_{ann}	7.5	4.4%	0.943	176.8	[100]	
181.0	46 $d\sigma_{el}$	48.7	5%	1.037	$\geq$0.925, #=6	[101,102]	j, o
183.0	13 $d\sigma_{ce}$	8.3	5%	0.976	0.940, −0.170, −0.574, −0.966	[103]	
194.8	19 $d\sigma_{el}$	.	4%	.	All	[104]	f, i, o
200.0– –588.2	48 σ_{ann}	57.8	2.2%	0.978		[100,105]	
221.9– –413.2	45 σ_{tot}	53.0	0.9%	0.971	221.9, 229.6	[106]	
233.0	54 $d\sigma_{el}$	87.6	5%	1.034	$\geq$0.938, #=6; 0.764	[107]	j
239.2	20 $d\sigma_{el}$	27.7	4%	1.089		[104]	o
272.0	65 $d\sigma_{el}$	55.9	5%	1.055	0.967	[107]	j
276.0– –922.0	21 σ_{ce}	32.0	5–10%	1.138		[108]	m
276.9	20 $d\sigma_{el}$	18.9	4%	1.042		[104]	o
287.0	54 $d\sigma_{el}$	.	5%	.	All	[101,102]	j, l, o
287.0	14 $d\sigma_{ce}$	24.0	5%	1.201	0.985	[103]	
310.4	20 $d\sigma_{el}$	30.1	4%	1.039		[104]	o
340.9	20 $d\sigma_{el}$	32.2	4%	1.044	−0.850	[104]	o
348.7	38 $d\sigma_{el}$	42.4	4%	0.993		[110]	i, o
355.0– –923.0	36 σ_{tot}	.	1.5%	.	All	[111]	e, m
353.3	119 $d\sigma_{el}$	116.4	5%	1.037	0.366	[112]	j, o
369.1	19 $d\sigma_{el}$	15.7	4%	1.020	0.550	[104]	i, o
374.0	39 $d\sigma_{el}$	24.3	5%	1.067		[113]	o
388.0– –598.6	29 σ_{tot}	35.4	0.7%	0.973		[114]	
392.4	19 $d\sigma_{el}$	.	5%	.	All	[115]	l
392.4	15 $d\sigma_{ce}$	.	5%	.	All	[116]	f
404.3	40 $d\sigma_{el}$	38.6	4%	0.994	−0.575, −0.925	[110]	i, o
406.0– –922.0	30 $d\sigma_{el}$	36.7	4%	0.896		[117]	n
406.0	119 $d\sigma_{el}$	99.8	5%	1.029	0.990, 0.750, 0.578	[112]	j, o
411.2	38 $d\sigma_{el}$	37.9	5%	1.025	−0.925	[113]	i, o
413.4	7 $d\sigma_{el}$	5.6	5%	1.054	0.992	[118]	j, o
424.5	7 $d\sigma_{el}$	.	5%	.	All	[118]	e, j, o
428.0	10 $d\sigma_{ce}$	12.3	20%	1.221		[119]	
435.8	7 $d\sigma_{el}$	1.6	5%	1.017	0.992	[118]	j, o
439.0	27 $d\sigma_{el}$	.	10%	.	All	[120]	l
439.0	24 $A_{y,el}$	38.8	5%	1.068	0.851	[120]	o
439.9	39 $d\sigma_{el}$	42.0	5%	1.031		[113]	o
440.8	38 $d\sigma_{el}$	61.4	5%	1.035		[113]	i, o
444.1	38 $d\sigma_{el}$	35.0	4%	0.972	0.175, −0.825, −0.875	[110]	i, o
446.0	119 $d\sigma_{el}$	115.3	5%	1.021		[112]	j, o
447.1	7 $d\sigma_{el}$	6.9	5%	1.050	0.992	[118]	j, o
458.3	8 $d\sigma_{el}$	2.0	5%	0.994	0.996	[118]	j, o
467.5	39 $d\sigma_{el}$	32.7	4%	1.039	−0.925	[110]	i, o
467.8	39 $d\sigma_{el}$	24.0	5%	1.056		[113]	o
469.2	8 $d\sigma_{el}$	8.2	5%	1.013	0.996	[118]	j, o
479.3	119 $d\sigma_{el}$	109.3	5%	1.003	0.919, 0.873, 0.697	[112]	j, o
480.0	10 $d\sigma_{ce}$	14.3	∞	1.154		[121]	g
481.2	8 $d\sigma_{el}$	7.2	5%	1.048	0.996	[118]	j, o
490.1	37 $d\sigma_{el}$	.	5%	.	All	[115]	l
490.1	15 $d\sigma_{ce}$	12.5	5%	1.068	−0.193	[116]	
490.6	39 $d\sigma_{el}$	47.5	5%	0.983		[113]	o
492.7	8 $d\sigma_{el}$	4.2	5%	1.014	0.996	[118]	j, o

TABLE I. *(Continued).*

p_{lab} (MeV/c)	No.[a] type[b]	χ^2_{min}	Norm error	Pred. norm[c]	Rejected[d]	Ref.	Comm.
497.0	14 $A_{y,el}$	7.3	∞	0.718		[122,123]	h
498.7	37 $d\sigma_{el}$	27.7	4%	1.004		[110]	i, o
503.8	8 $d\sigma_{el}$	13.3	5%	1.047	0.996	[118]	j, o
504.7	39 $d\sigma_{el}$	14.3	5%	1.021		[113]	o
505.0	54 $d\sigma_{el}$	.	5%	.	All	[101,102]	j, l, o
505.0	14 $d\sigma_{ce}$	30.1	5%	1.034	0.574	[103]	
508.0	119 $d\sigma_{el}$	105.3	5%	1.019	0.663, 0.530	[112]	j, o
508.9	39 $d\sigma_{el}$	28.7	5%	1.025		[113]	o
516.0	8 $d\sigma_{el}$	5.5	5%	1.018	0.996	[118]	j, o
523.0	15 $A_{y,el}$	8.3	∞	0.786		[122,123]	h
524.8	36 $d\sigma_{el}$	32.2	4%	1.020		[110]	i, o
525.9	39 $d\sigma_{el}$	45.0	5%	1.053		[113]	o
528.2	8 $d\sigma_{el}$	3.2	5%	1.005	0.996	[118]	j, o
533.6	119 $d\sigma_{el}$	133.7	5%	1.029		[112]	j, o
537.0	10 $d\sigma_{ce}$	19.4	∞	1.199		[121]	g
540.6	8 $d\sigma_{el}$	10.9	5%	1.015	0.996	[118]	j, o
543.2	39 $d\sigma_{el}$	38.4	5%	1.065	-0.975	[113]	o
544.0	33 $d\sigma_{el}$	.	10%	.	All	[120]	l
544.0	30 $A_{y,el}$	37.5	5%	1.046	≥ 0.883, #=3	[120]	o
546.0	23 $A_{y,ce}$	36.1	4%	0.959		[124]	
549.4	10 $d\sigma_{ce}$	7.1	20%	1.258		[119]	
550.0	67 $d\sigma_{el}$	76.0	5%	1.006	≥ 0.995, #=3; 0.910, 0.883, 0.869	[125]	j
553.1	34 $d\sigma_{el}$	38.6	4%	0.981		[110]	i, o
553.4	8 $d\sigma_{el}$	2.4	5%	1.017	0.996, 0.972	[118]	j, o
556.9	119 $d\sigma_{el}$	125.4	5%	1.025	0.908	[112]	j, o
558.5	39 $d\sigma_{el}$	45.4	5%	1.040		[113]	o
565.5	8 $d\sigma_{el}$	5.7	5%	1.006	0.996	[118]	j, o
568.4	37 $d\sigma_{el}$	34.3	5%	1.040	-0.675, -0.825	[113]	i, o
577.2	36 $d\sigma_{el}$	36.0	4%	0.983		[110]	i, o
578.1	9 $d\sigma_{el}$	6.2	5%	1.014	0.999	[118]	j, o
578.3	119 $d\sigma_{el}$	132.3	5%	1.047		[112]	j, o
584.0	10 $d\sigma_{ce}$	15.7	∞	1.112		[121]	g
590.0	39 $d\sigma_{el}$	.	5%	.	All	[101,102]	j, l, o
590.0	15 $d\sigma_{ce}$	32.8	5%	1.092	0.996, -0.574	[103]	
591.2	9 $d\sigma_{el}$	6.5	5%	1.029	0.999	[118]	j, o
591.2	39 $d\sigma_{el}$	.	5%	.	All	[115]	l
591.2	15 $d\sigma_{ce}$	18.0	5%	1.058	-0.358	[116]	
596.5	38 $d\sigma_{el}$	49.5	5%	1.075		[113]	o
599.2	33 $d\sigma_{el}$	15.8	4%	0.997		[110]	i, o
604.0	9 $d\sigma_{el}$	7.6	5%	0.987	0.998	[118]	j, o
615.0	38 $d\sigma_{el}$	48.1	5%	1.046	-0.575	[113]	o
617.0	9 $d\sigma_{el}$	6.7	5%	0.953	0.998	[118]	j, o
630.0	10 $d\sigma_{ce}$	9.3	∞	1.073		[121]	g
630.9	9 $d\sigma_{el}$	4.6	5%	0.997	0.998	[118]	j, o
639.6	38 $d\sigma_{el}$	17.1	5%	0.995	-0.175	[113]	o
644.7	9 $d\sigma_{el}$	7.8	5%	0.996	0.998	[118]	j, o
656.0	21 $A_{y,ce}$	21.9	4%	0.963		[124,126]	
658.1	38 $d\sigma_{el}$	37.4	5%	0.972	0.225, -0.675, -0.975	[113]	o
658.6	9 $d\sigma_{el}$	8.9	5%	1.004	0.998	[118]	j, o
670.0	10 $d\sigma_{ce}$	5.5	∞	1.165		[121]	g
671.5	9 $d\sigma_{el}$	3.3	5%	0.987	0.998	[118]	j, o
679.0	26 $d\sigma_{el}$	.	∞	.	All	[123]	l
679.0	27 $A_{y,el}$	23.1	∞	0.846	0.540	[122,123]	h
679.0	1 D_{yy}	1.4	$-$	.		[150]	p, q
679.1	4 $A_{y,el}$	6.3	5%	0.983		[127]	o
680.1	38 $d\sigma_{el}$	40.2	5%	1.003		[113]	o
686.1	9 $d\sigma_{el}$	3.9	5%	0.986	0.998	[118]	j, o
689.0	39 $d\sigma_{el}$	.	5%	.	All	[115]	l
689.0	16 $d\sigma_{ce}$	26.5	5%	1.010	-0.139	[116]	

TABLE I. *(Continued).*

p_{lab} (MeV/c)	No.[a] type[b]	χ^2_{min}	Norm error	Pred. norm[c]	Rejected[d]	Ref.	Comm.
690.0	89 $d\sigma_{el}$	103.5	4%	0.991	0.370	[128]	
693.0	34 $d\sigma_{ce}$	39.3	10%	1.069	−0.075	[126]	r
696.1	21 $d\sigma_{el}$	16.4	4%	1.026		[129]	
696.1	16 $d\sigma_{ce}$	21.0	4%	1.050		[129]	
697.0	24 $d\sigma_{el}$	.	10%	.	All	[130]	l
697.0	33 $A_{y,el}$	20.3	5%	1.022	0.629	[130]	o
698.0	10 $d\sigma_{ce}$	7.1	∞	1.237		[121]	g
700.0	4 $A_{y,el}$	2.1	5%	0.991		[131]	o
701.1	9 $d\sigma_{el}$	3.5	5%	1.000	0.998	[118]	j, o
715.3	9 $d\sigma_{el}$	10.6	5%	1.002	0.998	[118]	j, o
728.0	10 $d\sigma_{ce}$	2.9	∞	1.105		[121]	g
757.0	72 $d\sigma_{el}$	95.7	5%	1.055	≥0.996, #=3	[125]	j
767.0	22 $A_{y,ce}$	25.5	4%	1.113		[124]	
780.5	39 $d\sigma_{el}$	.	5%	.	All	[115]	l
780.5	15 $d\sigma_{ce}$	14.0	5%	0.974		[116]	
783.0	30 $d\sigma_{el}$	.	∞	.	All	[123]	l
783.0	30 $A_{y,el}$	30.1	4.5%	0.944	−0.300	[122,123]	
783.0	3 D_{yy}	4.9	–	.		[150]	p, q
790.0	95 $d\sigma_{el}$	101.5	4%	1.034		[128]	
860.0	95 $d\sigma_{el}$	70.5	4%	1.045	0.510	[128]	
875.0	23 $A_{y,ce}$	20.0	4%	0.995		[124]	
886.0	34 $d\sigma_{el}$	.	∞	.	All	[123]	l
886.0	34 $A_{y,el}$	38.5	4.5%	0.992		[122,123]	
886.0	1 D_{yy}	1.2	–	.		[150]	p, q
910.0	19 $d\sigma_{el}$	.	∞	.	all	[132]	f, g
910.0	21 $A_{y,el}$	14.7	5%	0.989		[132]	

[a]The number includes all published data, except those given as 0.0±0.0 (see i), and those having $p_{lab} > 925$ MeV/c (see m).

[b]The subscripts "el" and "ce" denote observables in the elastic $\bar{p}p \rightarrow \bar{p}p$ and charge-exchange $\bar{p}p \rightarrow \bar{n}n$ reactions, respectively. "$d\sigma$" denotes a differential cross section $d\sigma/d\Omega$, A_y a polarization-type datum (asymmetry or analyzing power), and D_{yy} a depolarization datum. σ_{tot} stands for total cross section, σ_{ann} for (total) annihilation cross section, and σ_{ce} for integrated charge-exchange cross section.

[c]Normalization, predicted by the analysis, with which the experimental values should be multiplied before comparison with the theoretical values.

[d]Tabulated is p_{lab} in MeV/c or $\cos\theta$. The notation "≥0.925, #=6," e.g., means that the 6 points with $\cos\theta \geq 0.925$ are rejected.

[e]Group rejected due to improbable low χ^2_{min}.

[f]Group rejected due to improbable high χ^2_{min}.

[g]Floated normalization. Data are relative only.

[h]Normalization floated by us, since the norm contributes much more than 9 to χ^2_{min}.

[i]Data points given as 0.0±0.0 not included.

[j]Coulomb-nuclear-interference measurement. Data points in the extreme forward angular region are rejected when they contain multiple-scattering effects.

[k]Data points at low momenta rejected (see text).

[l]Problematic differential cross section. Not included in the database. See the text, Sec. VIII B and Tables II and III.

[m]Part of a group of data with points having $p_{lab} > 925$ MeV/c.

[n]Elastic differential cross sections as a function of momentum taken at backward angle $\cos\theta = -0.994$.

[o]Normalization error assumed by us, since no clear number is stated in the reference.

[p]Depolarization data. Not included in the fit, in view of large error bars.

[q]Normalization error taken to be zero, in view of large error bars of these data.

[r]Data points taken at the same angles averaged.

been PS199 whose goal was to study the spin structure of the charge-exchange reaction. So far, it has obtained very accurate data on the differential charge-exchange cross section at 693 MeV/c and very important data on the charge-exchange analyzing power A_y between 546 and 875 MeV/c [126,124]. More results from PS199 can be expected in the near future. Very recently, a new LEAR experiment called PS206 [153] has been approved that will further study the charge-exchange reaction.

B. Flaws in elastic differential cross-section data

Since 1983 several experiments have measured the elastic differential cross section at different momenta. PS173 at LEAR measured this observable at low momenta between 181 and 590 MeV/c [101,102]. It was subsequently measured at KEK between 392 and 781 MeV/c [115], by PS172 at 679, 783, and 886 MeV/c [123] (and at higher energies), and by PS198 at 439, 544, and 697 MeV/c [130,120]. Unfortunately, these different experiments do not appear to be consistent with each other, nor with the accurate pre-LEAR data of Eisenhandler *et al.* [128] which are described very well in the PWA. In fact, this is the most serious flaw in the $\bar{p}p$ database and a major obstacle in fitting potential models [25]. It is

highly probable that some of these data contain unspecified systematic errors, or that the statistical errors have been underestimated.

Since we are talking about a total of 540 cross sections (not counting the Eisenhandler data) we decided to put some effort in trying to determine what is wrong with these data, instead of rejecting them outright. This turned out to be very difficult. The discussion about statistical and systematic errors in most of the original papers can be called marginal at best. Sometimes results from Legendre fits are presented, but in several cases it turns out that the $\chi^2_{\min}$ of these fits is much too high for a statistical data set. The procedure that we followed to examine these data was as follows. We fitted each differential cross section with

$$d\sigma/d\Omega = \sum_{\ell=0}^{\ell_{max}} a_\ell P_\ell(\cos\theta) \ .$$

ℓ_{max} was determined by the requirement that the error on the corresponding coefficient a_ℓ was smaller than the coefficient itself. In the ideal situation this would give a fit with $\chi^2_{\min}/N_{df} \approx 1.0$. However, for few groups this was actually the case. We then enlarged the errors by adding a point-to-point systematic error in quadra-

TABLE II. Corrections applied to elastic differential cross sections from Eisenhandler *et al.*, from PS172, PS173, and PS198 from LEAR, and from KEK. The number of data includes all published points. The column labeled "syst. error" gives the approximate point-to-point error that has to be added quadratically to the statistical error to reach $\chi^2_{\min} \approx N_{df}$. The column labeled "$\chi^2_{unc}$" gives the result of the Legendre fit without any corrections, except that PS173 points at forward angles contaminated by multiple-scattering effects are removed. For the values of $\chi^2_{\min}$ after the corrections, see Table III.

p_{lab} (MeV/c)	Group	No. data	Rejected points ($\cos\theta$)	Syst. error	χ^2_{unc}	Ref.	Comm.
181.0	PS173	46	> 0.92, #=6		41.0	[101,102]	a
287.0	PS173	54	> 0.95, #=9; 0.345, 0.199, 0.101, 0.051, -0.345	5%	160.7	[101,102]	a
392.4	KEK	19		2%	19.2	[115]	b
439.0	PS198	27		4%	28.0	[120]	
490.1	KEK	18		4%	202.0		b
		19			15.0	[115]	c
505.0	PS173	54	> 0.98, #=3; 0.96, 0.67		59.5	[101,102]	a
544.0	PS198	33			23.1	[120]	
590.0	PS173	39	> 0.99, #=2	3%	39.0	[101,102]	a
591.2	KEK	19	0.825	3%	276.2		b
		20	0.275, -0.075	2%	36.0	[115]	c
679.0	PS172	26	0.50, -0.50		82.7	[123]	d
689.0	KEK	15		3%	90.5		b
		24		3%	24.2	[115]	c
690.0	Eisenh.	89	0.37		101.9	[128]	
697.0	PS198	24		6%	174.0	[130]	
780.5	KEK	14		2%	30.5		b
		25			16.4	[115]	c
783.0	PS172	30	0.58, -0.58		31.9	[123]	d
790.0	Eisenh.	95			88.2	[128]	
860.0	Eisenh.	95			69.4	[128]	
886.0	PS172	34	0.66, 0.54, 0.46, -0.18, -0.66		77.6	[123]	d

[a]Data points in the extreme forward angular region are rejected because they contain multiple-scattering effects.
[b]Data in the "one-prong" region. For a discussion, see the text.
[c]Data in the "two-prong" region. For a discussion, see the text.
[d]The most forward and the most backward data point are rejected (Bradamante, private communication).

ANTIPROTON-PROTON PARTIAL-WAVE ANALYSIS BELOW . . .

ture to the quoted statistical errors. The amount of error added was determined by the requirement that now indeed $\chi^2_{\min} \approx N_{\text{df}}$. Once for a group this result was approached, outliers were removed (three-standard-deviation rule). For some groups special measures had to be taken, which we will discuss now. The results of these investigations are summarized in Table II.

The data measured by PS173 [101,102] are at the most forward angles contaminated by effects due to multiple scattering in the target (Molière scattering). Since the experimentalists do not present their data corrected for these effects, and since these corrections depend on details of the target used, there is no way for us to take these effects into account. Consequently, the only sensible thing to do is to reject the data at angles where multiple-scattering effects are believed to be seen. These data were used to extract the real-to-imaginary ratio of the forward-scattering amplitude [148]. It is perhaps remarkable that in Ref. [148] values for this ratio were presented at more momenta than the four for which the corresponding differential cross sections were presented in Refs. [101,102]. These remaining cross sections have never been published. After removing the points at forword angles, difficulties remain. At 287 MeV/c it is necessary to reject five individual data points and add a 5% point-to-point error. At 505 MeV/c two outliers must be removed and at 590 MeV/c a 3% error must be added.

The data taken at KEK [115] present serious difficulties of a different kind. The only manner to achieve satisfactory results in a Legendre fit seemed to be to either reject a large number of data points or to enlarge all errors by

a significant amount ($\approx 6-7\%$). However, improvement could be obtained in the following manner. It turned out that most difficulties resided in the data taken in the "one-prong" region [115], i.e., at forward and backward angles. The data at intermediate angles, the "two-prong" region, appear to be less troublesome. In fact, in Ref. [115] different systematic errors are quoted for these two regions, although the experimentalists perform Legendre fits to the data as one group. When we split the groups at 490, 591, 689, and 781 MeV/c into two different parts, it suffices to enlarge the statistical errors by a smaller amount, and in some "two-prong" regions the data need no corrections at all.

The description of the data taken by PS172 [123] improves when the points at the most forward and at the most backward angle are removed at all momenta (Bradamante, private communication). At 886 MeV/c three additional outliers have to be rejected. Especially for these groups there remains a big problem with the normalization [123] (see below). For the data at 697 MeV/c [130] from the PS198 group the statistical errors may have been underestimated. We had to enlarge these by adding a 6% point-to-point error.

After all these corrections have been applied to the different groups the next step is to see to what extent the Legendre coefficients at comparable momenta are consistent. These coefficients are presented in Table III. It is immediately clear that significant problems occur in the normalization a_0 of the different groups (which is why we present the "renormalized" Legendre coefficients a_ℓ/a_0 for $\ell > 0$). This is especially true for the PS172 data.

TABLE III. Legendre-polynomial fits to elastic differential cross sections from Eisenhandler *et al.*, PS172, PS173, and PS198 from LEAR, and from KEK. The corrections summarized in Table II are taken into account. The number of data is the number of published data minus the rejected points. For the KEK groups at 490, 591, 689, and 781 MeV/c the first line gives the results for the "one-prong" region, and the second line the results for the "two-prong" region.

p_{lab} (MeV/c)	Group	No. data	a_0	a_1/a_0	a_2/a_0	a_3/a_0	a_4/a_0	a_5/a_0	a_6/a_0	$\chi^2_{\min}$
181.0	PS173	40	7.02(25)	0.92(06)	0.46(07)					41.0
287.0	PS173	40	5.10(07)	1.58(03)	0.82(03)	0.15(02)				36.0
392.4	KEK	19	5.49(06)	1.92(04)	1.35(05)	0.35(03)				15.6
439.0	PS198	27	4.09(08)	1.93(06)	1.63(07)	0.67(08)	0.39(09)	0.19(07)	0.09(04)	19.6
490.1	KEK	18	5.07(10)	1.95(05)	1.55(07)	0.50(05)	0.10(03)			15.4
		19	5.61(45)	1.91(21)	1.89(28)	0.72(13)	0.38(10)			15.0
505.0	PS173	49	4.18(05)	1.90(04)	1.76(04)	0.96(05)	0.49(06)	0.11(05)	0.06(04)	36.1
544.0	PS198	33	3.79(05)	2.08(05)	2.16(06)	1.16(06)	0.57(06)	0.12(04)	0.04(02)	23.1
590.0	PS173	37	3.73(06)	2.11(05)	2.09(05)	1.25(06)	0.66(06)	0.26(05)	0.10(03)	32.2
591.2	KEK	18	4.42(08)	2.12(05)	1.95(06)	0.83(04)	0.16(03)			13.8
		18	5.24(33)	2.07(18)	2.08(22)	0.99(11)	0.38(07)			15.2
679.0	PS172	24	1.96(02)	2.59(05)	1.88(02)	1.39(04)				18.8
689.0	KEK	15	3.52(22)	2.27(15)	2.35(18)	1.46(11)	0.63(14)	0.17(07)		9.8
		24	3.21(15)	2.16(14)	2.14(17)	1.20(09)	0.38(06)			19.0
690.0	Eisenh.	88	4.28(07)	2.28(06)	2.45(08)	1.67(07)	0.76(06)	0.23(04)	0.03(02)	81.6
697.0	PS198	24	3.54(09)	2.22(08)	2.30(09)	1.43(08)	0.51(05)	0.10(02)		21.5
780.5	KEK	14	3.14(23)	2.37(17)	2.72(23)	2.10(16)	1.07(16)	0.29(07)		9.1
		25	2.39(10)	2.07(11)	2.39(16)	1.36(08)	0.66(07)			16.4
783.0	PS172	28	2.55(07)	2.73(17)	2.45(11)	2.26(20)	0.67(05)	0.38(07)		29.8
790.0	Eisenh.	95	3.87(08)	2.36(07)	2.69(09)	2.08(09)	1.09(07)	0.42(05)	0.12(03)	88.2
860.0	Eisenh.	95	3.67(06)	2.41(06)	2.83(07)	2.33(07)	1.34(05)	0.56(04)	0.17(02)	69.4
886.0	PS172	29	2.44(04)	2.66(08)	2.64(06)	2.46(09)	0.95(03)	0.47(04)		22.2

The probable reason [123] for the difficulties is that data could only be taken in a very limited angular region, so that only a small fraction $\approx 5\%$ of the cross section is detected. Properly normalizing the data is then especially difficult. These data would have to be treated with a "floated" normalization. Certainly a 10% normalization uncertainty as suggested in Ref. [123] is not sufficient. Since also the KEK data in the "two-prong" region cover a limited angular region it would be a good idea to float these normalizations as well, since they are not consistent with the normalizations of the data in the "one-prong" regions. Apart from these normalization problems it is clear from a study of Table III that it is very unlikely that the different experiments are consistent. Certainly, the PS173 data at 590 MeV/c are not compatible with the KEK data at 591 MeV/c; the PS172 data at 783 MeV/c are not compatible with the KEK data at 781 MeV/c, nor with the Eisenhandler data at 790 MeV/c. The PS198 data at 439 MeV/c do not appear to intrapolate between the KEK data at 392 and 490 MeV/c, etc. So, although many beautiful data have come out of LEAR and KEK, unfortunately elastic differential cross sections are not among them.

To summarize, at present we are prejudiced in favor of the pre-LEAR data by Eisenhandler et al. [128], although we cannot exclude completely the possibility that these data contain unspecified systematic errors and that one of the LEAR or (more unlikely) the KEK experiments is correct after all. Preliminary study showed that we could obtain a reasonable fit to the LEAR data from PS172 and PS198, but only at the cost of rejecting the pre-LEAR data of Eisenhandler et al. [128] and of Sakamoto et al. [113]. And still, the problems with the data from PS173 and KEK would remain. Further investigation is required before such a drastic step will be taken. Obviously, a dedicated new experiment that might shed some light on this issue would be highly welcome.

IX. RESULTS

After deciding on the final content of the Nijmegen 1993 $\bar{p}p$ database to be used in the PWA, the free P-matrix parameters are fitted to these data.[1] In Table I we present an overview of the results of this fit for all the $\bar{p}p$ scattering data. In this table one can find the values for $\chi^2_{\min}$ for each individual group, the normalization predicted by the PWA, and the data points and groups that have been rejected by us on statistical grounds. The total number of scattering observables that are rejected is 204, not including the problematic LEAR and KEK elastic differential cross sections discussed in the previous section. Three normalization data are rejected. We reject three groups because of an improbable high $\chi^2_{\min}$,

---

[1] For the sake of completeness we mention that at the time of our final fit, the data of Refs. [151,152,147] were not available to us. Also, we were at that time not aware of the existence of the data of Refs. [136,137].

and two groups because of an improbable low $\chi^2_{\min}$. In the final fit we have (in the notation of Sec. VII)

$$N_{\text{obs}} = 3543, \quad N_n = 113, \quad N_{\text{ne}} = 103, \quad N_{\text{par}} = 30,$$

so that

$$N_{\text{data}} = 3646, \quad N_{\text{fp}} = 143, \quad N_{\text{nf}} = 10, \quad N_{\text{df}} = 3503.$$

When the data set is a perfect statistical ensemble and when the model is totally correct one expects

$$\langle \chi^2_{\min}/N_{\text{df}} \rangle = 1.000 \pm 0.024.$$

Our best fit to the final 1993 database results in

$$\chi^2_{\min} = 3801.0,$$

corresponding to

$$\chi^2_{\min}/N_{\text{data}} = 1.043 \quad \text{and} \quad \chi^2_{\min}/N_{\text{df}} = 1.085.$$

The 3543 scattering observables contribute 3700.9 to $\chi^2_{\min}$, which means that the 103 normalization data contribute the remaining 100.1 of $\chi^2_{\min}$.

In order to get a feeling for some of these numbers, let us compare them to the NN case. In the Nijmegen NN PWA the database contains $N_{\text{data}} = 4301$ NN scattering data, which are described with $\chi^2_{\min} = 4263.8$ or $\chi^2_{\min}/N_{\text{data}} = 0.991$ [7]. The number of model parameters needed in our case is 30, which is a reasonable number, in view of the fact that 21 parameters were used in the Nijmegen pp PWA and an additional 18 in the np PWA.

The values for the P-matrix parameters and their errors are tabulated in Table IV. The parameters for the higher partial waves are the same as the corresponding state given in this table. For instance, the $^1F_3$ wave has

TABLE IV. P-matrix parameters of the different partial waves. V_0 and V_1 are the real parts of the short-range spherical-well potential, for isospin $I = 0$ and $I = 1$, respectively. W is the isospin-independent imaginary part. The mixing angles that take care of the short-range $I = 0$ tensor force are $\theta_1 = 55.7° \pm 1.3°$ for the $^3C_1$ state, $\theta_2 = 45.8° \pm 1.1°$ for the $^3C_2$ state, and $\theta_2 = 10.7° \pm 4.7°$ for the $^3C_3$ state. The quoted errors are defined as the change in each parameter that gives a maximal rise in $\chi^2_{\min}$ of 1 when the remaining parameters are refitted.

Partial wave	V_0 (MeV)	V_1 (MeV)	W (MeV)
$^1S_0$	0	0	$-99(6)$
$^3S_1$	$-151(6)$	$-17(3)$	$-100(3)$
$^1P_1$	0	0	$-90(7)$
$^3P_0$	$-132(9)$	$178(19)$	$-156(9)$
$^3P_1$	$155(12)$	$-66(3)$	$-97(4)$
$^3P_2$	$-136(4)$	$-69(3)$	$-142(3)$
$^1D_2$	0	0	$-105(12)$
$^3D_1$	$-215(7)$	$33(16)$	$-106(5)$
$^3D_2$	$-38(12)$	$-198(4)$	$-110(4)$
$^3D_3$	$-152(6)$	$-102(5)$	$-163(4)$
$^3F_2$	$-101(20)$	$-250(14)$	$-179(7)$

the same parameters as the $^1D_2$ wave, the $^3F_3$ wave the same as the $^3D_2$ wave, the $^3G_3$ the same as the $^3F_2$, and so on. This is just a convenient prescription. For higher partial waves the short-range parametrization is irrelevant due to the centrifugal barrier and the dynamics is completely determined by the potential tail. As explained in Sec. III, these parameters correspond to a spin-dependent optical potential for the short-range interaction. It can be seen that even if one introduces for each partial wave of specific isospin a simple complex spherical-well potential, then still by no means all of these parameters can be determined from the existing data. This is in striking contrast with for instance the pp analysis where one needs four parameters already to describe the $^1S_0$ channel. The reason is that the pp $^1S_0$ phase shift is very accurately known at very low energies (below 3 MeV). A proper description of the P waves in the pp case also requires more than one parameter for each wave. In our $\bar{p}p$ case, no single partial wave (of specific isospin) needs more than one parameter for the real part of the short-range interaction, but, on the other hand, many more partial waves contribute significantly to the scattering process. This is especially true for the charge-

exchange reaction, as can be seen from Table V where we give the partial-wave cross sections for the elastic and charge-exchange reaction at a number of momenta, as well as the total and annihilation cross section. Compared to nucleon-nucleon scattering, one notes a large contribution of P and D waves to the cross sections already at low momenta. The reason for this is the greater strength of the antinucleon-nucleon potentials, especially the central and tensor potentials.

In Fig. 1 we show the results for the total and annihilation cross sections as a function of momentum. The high-quality data are from the LEAR experiments PS172 [106,114] (total cross sections) and PS173 [105,100] (annihilation cross sections). We calculate total cross sections with the optical theorem. Obviously, these cross sections can only be compared to the experimental data, when the effects of the Coulomb interaction can be neglected. Except for the lowest momenta ($p_{lab} < 200$ MeV/c) this is probably a good approximation. An example of the fit to the differential cross sections from Eisenhandler et $al.$ [128] is shown in Fig. 2. In Fig. 3 the fit to the backward elastic cross sections ($\cos\theta = -0.994$) from Ref. [117] is demonstrated. As-

TABLE V. Partial elastic and charge-exchange cross sections in mb.

p_{lab} (MeV/c)	$\bar{p}p \to \bar{p}p$				$\bar{p}p \to \bar{n}n$			
	200	400	600	800	200	400	600	800
$^1S_0$	14.6	6.8	3.7	1.9	0.5			
$^1P_1$	1.7	2.6	2.5	2.4	1.3	0.4		
$^1D_2$	0.1	0.4	0.7	0.8	0.1	0.4	0.2	
$^1F_3$			0.1	0.2		0.1	0.1	0.1
$^1G_4$				0.1			0.1	0.1
$^3P_1$	1.8	7.6	7.6	6.2	6.7	6.2	2.8	1.4
$^3D_2$	0.1	0.3	2.2	3.9	0.3	2.6	3.2	2.0
$^3F_3$		0.1	0.1	0.2		0.4	1.0	1.4
$^3G_4$							0.3	0.4
$^3P_0$	4.7	4.6	3.4	2.6	2.1	1.4	0.7	0.3
$^3S_1$	71.1	29.6	14.4	7.9	2.0	0.5	0.3	0.3
$^3S_1 \to {}^3D_1$	0.2	0.1			0.6	0.5	0.1	
$^3D_1 \to {}^3S_1$	0.2	0.1			1.4	0.7	0.1	
$^3D_1$		0.3	0.8	1.3	0.1	0.3	0.5	0.4
$^3P_2$	6.3	16.1	15.5	12.9	0.8	1.2	0.5	0.3
$^3P_2 \to {}^3F_2$	0.1	0.1	0.2	0.2	0.1	0.4	0.4	0.2
$^3F_2 \to {}^3P_2$	0.1	0.1	0.2	0.2	0.3	0.6	0.4	0.3
$^3F_2$			0.1	0.3				0.1
$^3D_3$		1.2	5.0	7.1		0.4	1.0	0.6
$^3D_3 \to {}^3G_3$		0.1	0.1	0.1		0.2	0.3	0.2
$^3G_3 \to {}^3D_3$		0.1	0.1	0.1		0.3	0.4	0.3
$^3G_3$								0.1
$^3F_4$			0.3	1.2			0.1	0.1
$^3F_4 \to {}^3H_4$				0.1			0.1	0.2
$^3H_4 \to {}^3F_4$				0.1		0.1	0.2	0.2
$^3H_4$								
Rest	0.1	0.1	0.1	0.1	0.1	0.1	0.1	0.9
Singlet	16.4	9.8	7.0	5.4	2.0	0.9	0.4	0.2
Triplet	84.7	60.5	50.1	44.5	14.4	15.9	12.6	9.6
Total	101.1	70.3	57.1	49.9	16.4	16.8	13.0	9.8

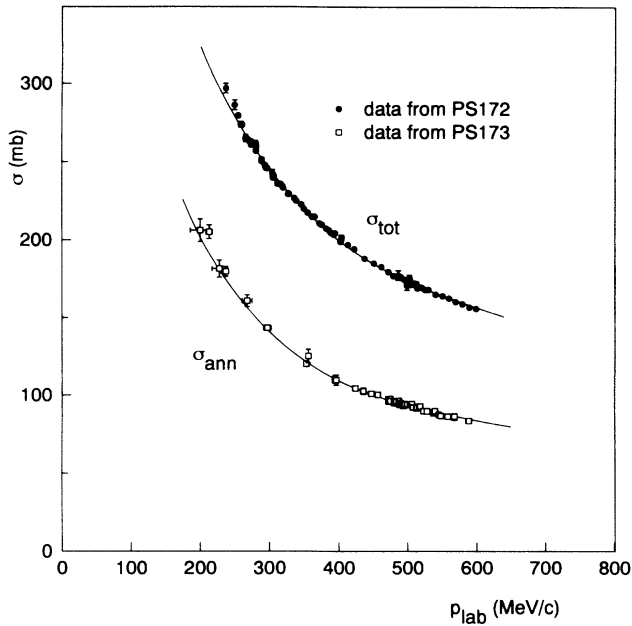| p_{lab} (MeV/c)	$\bar{p}p \to$ all				$\bar{p}p \to$ mesons			
	200	400	600	800	200	400	600	800
	314.7	193.9	151.8	128.5	197.2	106.8	81.7	68.8

FIG. 1. Total and annihilation cross section as a function of momentum in antiproton-proton scattering. The σ_{tot} data are from the LEAR experiment PS172 [114,106] and the σ_{ann} data are from experiment PS173 [105,100]. The curve from the PWA for σ_{tot} has $\chi^2_{min} = 88.4$ for 75 points, and the curve for σ_{ann} has $\chi^2_{min} = 65.3$ for 52 points.

suming that these data are correct, it can be seen from this figure that there appears to be room for improvement at the lowest momenta. This is precisely the momentum region ($p_{lab} \approx 509$ MeV/c) where some statistical evidence for a resonance was found [138]. The differential cross section for charge-exchange scattering is given in

FIG. 3. Elastic cross section at backward angle $\cos \theta = -0.994$ as a function of momentum. The data are from Alston-Garnjost et al. [117]. The curve from the PWA has $\chi^2_{min} = 36.7$ for 30 points.

Fig. 4, compared to recent high-quality data taken by PS199 [126] at 693 MeV/c. This is one of the most constraining experiments in the database. In order to fit this group properly, orbital angular momenta up to $\ell = 10$ must be taken into account. The cross section exhibits the typical dip-bump structure at forward angles, which can be understood as an interference effect between one-

FIG. 2. Differential cross section for elastic scattering at 790 MeV/c. The data are from Eisenhandler et al. [128]. The curve from the PWA has $\chi^2_{min} = 101.5$ for 95 points.
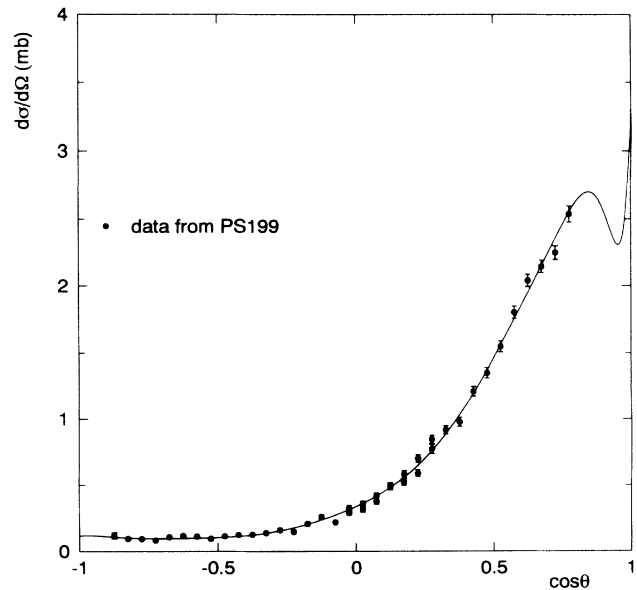
FIG. 4. Differential cross section for charge-exchange scattering at 693 MeV/c. The data are from the LEAR experiment PS199 [126]. The curve from the PWA has $\chi^2_{min} = 39.3$ for 33 points.

pion exchange and a background [154]. Unfortunately, no data of similar quality have been taken in this dip-bump region.

In Fig. 5 we give the results for the analyzing power (polarization) for elastic scattering, compared with the recent data from PS172 [122] and from PS198 [130,120]. The fits to the analyzing-power data for the charge-exchange reaction from PS199 [126,124] are shown in Fig. 6. Finally, in Fig. 7 the prediction for the depolarization for elastic scattering at 783 MeV/c is shown compared to the data from PS172 [150]. Only a few depolarization data exist: one point at 679 MeV/c, three points at 783 MeV/c, and one point at 886 MeV/c. These data points are not included in the fit in view of the large

error bars. This also means that no normalization error is taken into account.

In Sec. VI a formalism was proposed to extract phase-shift parameters and inelasticities from the S matrix for antinucleon-nucleon scattering. It does not make much sense to present all these phase shifts, inelasticities, and mixing parameters without a proper assessment of the uncertainties (statistical errors). This, however, requires a lot of work. Preliminary study shows that the phase-shift parameters for the $^1S_0$ and $^1P_1$ partial waves are not pinned down accurately at all above $p_{\rm lab} \approx 400$ MeV/c. On the other hand, a large number of parameters appear to be very well determined by the existing data, such as the $^3P_{0,1,2}$ and $^3D_{2,3}$ phase shifts and inelasticities,
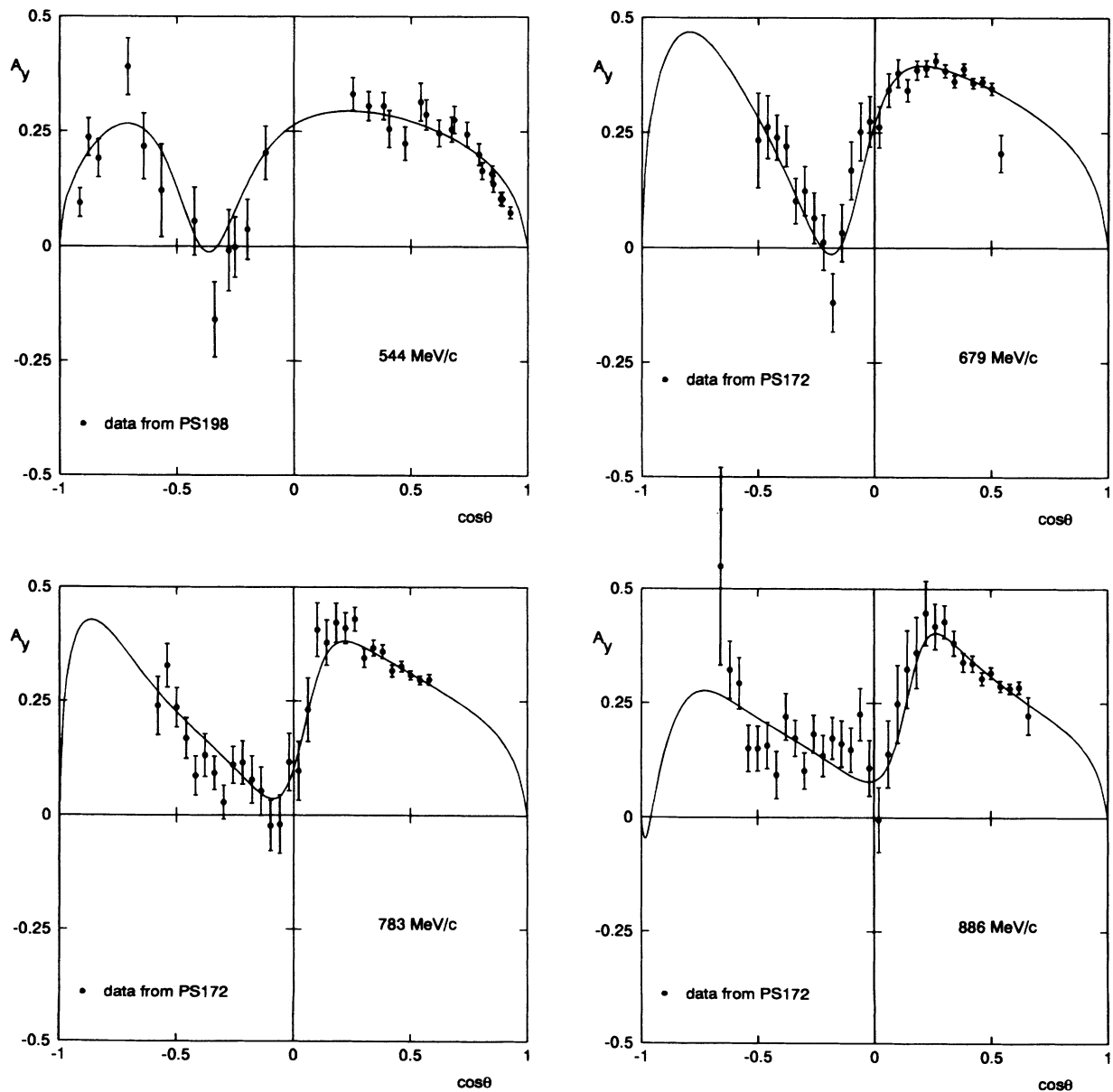
FIG. 5. Analyzing power in elastic scattering at 544, 679, 783, and 886 MeV/c. The data are from the LEAR experiments PS172 [122] and PS198 [120]. The curves from the PWA have $\chi^2_{\rm min} =37.5$, 23.1, 30.1, and 38.5 for 27, 26, 29, and 34 points, respectively.

and the $\varepsilon_{1,2}$ mixing parameters. All results are available in numerical form from the authors. An extensive discussion of the remaining uncertainties in the predictions of the PWA and the phase-shift parameters will be presented elsewhere.

In our 1991 preliminary PWA [29] we were able to determine the charged-pion-nucleon coupling constant f_c^2 from the data on the charge-exchange reaction $\bar{p}p \to \bar{n}n$, in which only isovector mesons can be exchanged. In this PWA we analyzed 884 scattering observables between 400 and 950 MeV/c, using 23 free parameters. We found f_c^2 = 0.0751(17), at the pion pole. The error is purely statistical. This value was in nice agreement with other determinations of f_c^2 from np [155] and $\pi^{\pm}p$ scattering

data [156]. These results provided strong evidence for an approximate charge-independent pion-nucleon coupling constant, since they were consistent with the value for f_p^2 found in the Nijmegen pp PWA [6].

Since this preliminary analysis, more high-quality analyzing-power data for the charge-exchange reaction have become available from PS199 [124]. We have repeated the determination of f_c^2, but this time from the complete 1993 Nijmegen database. The coupling constants of the neutral pion were kept at the value of f_p^2 = f_n^2 = 0.0745. Since f_p^2 is determined by the data on elastic scattering $\bar{p}p \to \bar{p}p$, and f_c^2 by the data on charge-exchange scattering $\bar{p}p \to \bar{n}n$, one expects that the cor-
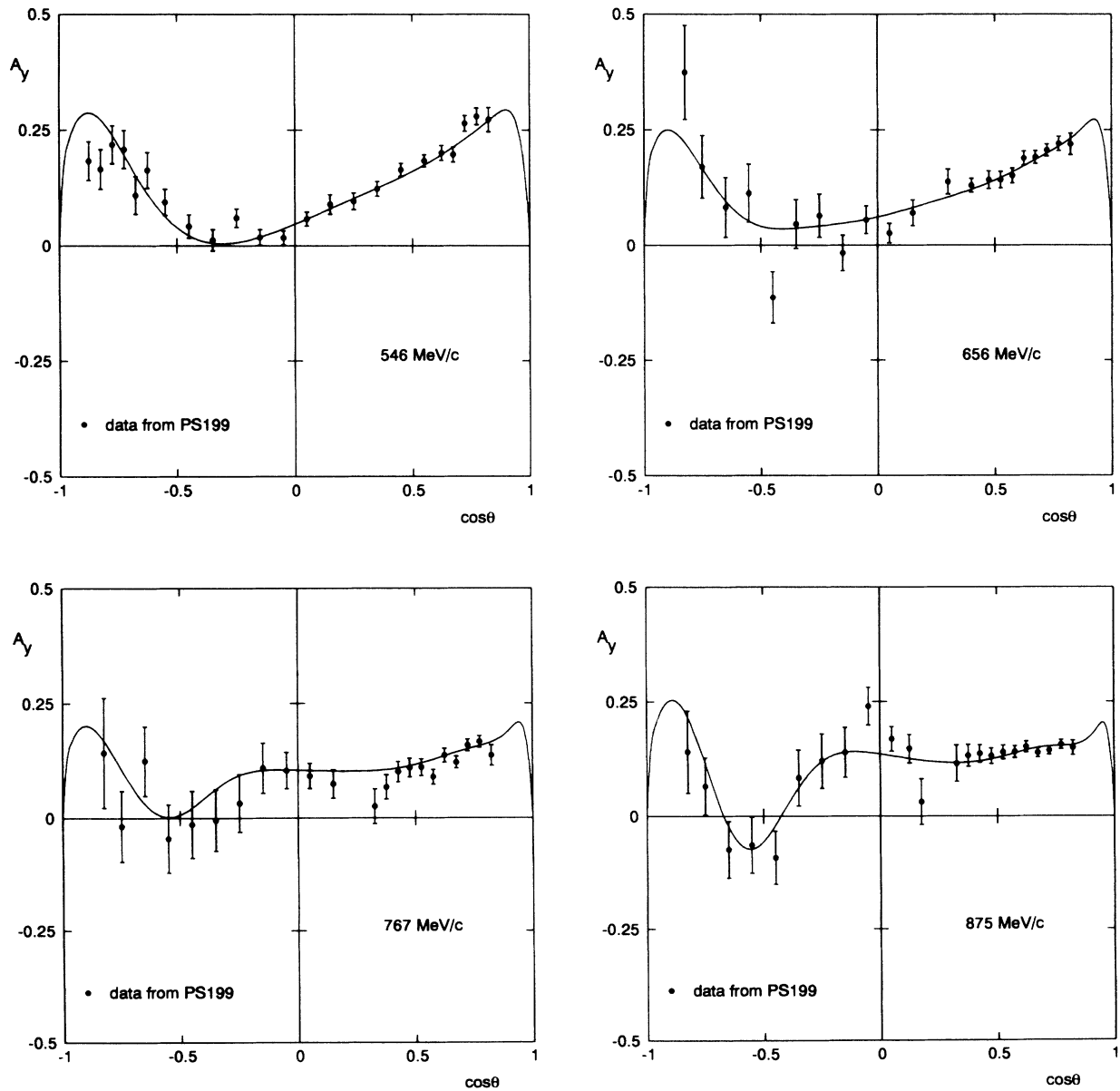
FIG. 6. Analyzing power in charge-exchange scattering at 546, 656, 767, and 875 MeV/c. The data are from the LEAR experiment PS199 [126,124]. The curves from the PWA have χ^2_{min} =36.1, 21.9, 25.5, and 20.0 for 23, 21, 22, and 23 points, respectively.
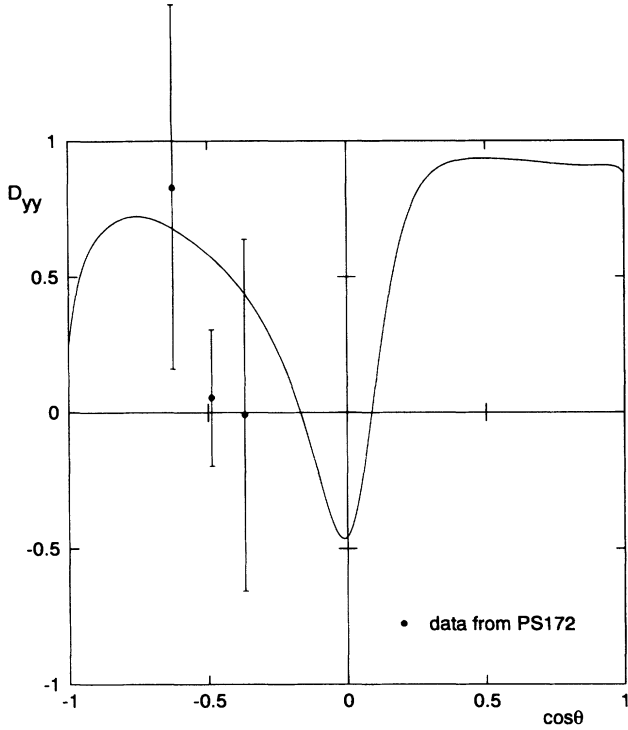
FIG. 7. Depolarization in elastic scattering at 783 MeV/c. The data are from the LEAR experiment PS172 [150]. The curve from the PWA has $\chi^2_{\min} = 4.9$ for 3 points.

relation between the two is small. Adding f_c^2 as the 31st free parameter, we now find

$$f_c^2 = 0.0732(11) \ ,$$

at the pion pole. This result supersedes our previous value from Ref. [29]. Again, the error is of statistical origin only. In view of the enormous amount of work involved, it is very hard for us to make statements about possible systematic errors on this result. In Ref. [29] we did demonstrate that there were no systematic errors due to form-factor effects or due to $\rho(770)$ exchange. In the Nijmegen pp PWA systematic errors could be more thoroughly investigated and there they were found to be small [60]. Although in our case the systematic errors are probably larger than for the pp case, it is very encouraging that the available charge-exchange data pin down the charged-pion coupling constant with a remarkably small statistical error and that the result is consistent with other determinations from $\pi^{\pm}p$ [156] and NN scattering [155,60]. Very probably the new LEAR experiment PS206 [153] will further constrain the charged-pion-nucleon coupling constant.

X. SUMMARY OF CONCLUSIONS

To summarize, we have performed an energy-dependent partial-wave analysis of all antiproton-proton scattering data below 925 MeV/c antiproton momentum, published in a regular physics journal since 1968. This is

the first time such an analysis has been attempted. We have set up the Nijmegen 1993 $\bar{p}p$ database by scrutinizing and passing sentence on all available $\bar{p}p$ scattering observables below 925 MeV/c. Serious problems were encountered with a set of 540 elastic differential cross sections from LEAR and KEK. These data were rejected, although further study is required here. Of the remaining 3747 scattering observables 204 (5.4%) were rejected on the grounds of sound statistical criteria. We also rejected three normalization data. The final database contains 3543 scattering observables and 103 normalization data for a total of 3646 scattering data. Using 30 free parameters we obtain $\chi^2_{\min} = 3801.0$ corresponding to $\chi^2_{\min}/N_{\mathrm{data}} = 1.043$. This shows that the tail of the charge-conjugated Nijmegen potential is a realistic intermediate- and long-range $\bar{p}p$ force. Data on the charge-exchange reaction $\bar{p}p \rightarrow \bar{n}n$ provide further evidence for a "low" and approximately charge-independent pion-nucleon coupling constant $f_{NN\pi}^2 \approx 0.0745$. The present results will serve as a starting-point for future investigations by our group of the antiproton-proton system, and should be of help in planning further experiments at LEAR and elsewhere.

ACKNOWLEDGMENTS

APPENDIX: FROM S MATRIX TO PHASE PARAMETERS

In his second paper on the subject of parametrizing the S matrix for nucleon-nucleon scattering above the pion-production threshold [94], Bryan has presented an easy algorithm to extract the three parameters $\bar{\delta}_{J-1,J}$, $\bar{\delta}_{J+1,J}$, ε_J, and the three different elements of the inelasticity matrix H^J from the 2×2 S matrix, written as

$$S^J = \exp(i\bar{\delta}) \exp(i\bar{\varepsilon}_J \sigma_x) \, H^J \exp(i\bar{\varepsilon}_J \sigma_x) \exp(i\bar{\delta}) \ .$$

$$(A1)$$

For completeness we list the relevant expressions. The derivation can be found in the paper by Bryan. If the S matrix is presented numerically as

$$S^J = \begin{pmatrix} R_{11}\exp(2i\delta_{11}) & iR_{12}\exp(2i\delta_{12}) \\ iR_{12}\exp(2i\delta_{12}) & R_{22}\exp(2i\delta_{22}) \end{pmatrix} \ , \quad (A2)$$

then the phase shifts $\bar{\delta}_{J-1,J}$ and $\bar{\delta}_{J+1,J}$ can be obtained from the following two equations:

$$\tan 2(\theta_a + \theta_b) = \frac{R_{12}^2 \sin 2\delta}{R_{11}R_{22} + R_{12}^2 \cos 2\delta} , \qquad (A3)$$

$$\tan(\theta_a - \theta_b) = \frac{R_{22} - R_{11}}{R_{11} + R_{22}} \tan(\theta_a + \theta_b) . \qquad (A4)$$

Here we defined the auxiliary phases

$$\theta_a \equiv \delta_{11} - \bar{\delta}_{J-1,J} , \qquad (A5)$$

$$\theta_b \equiv \delta_{22} - \bar{\delta}_{J+1,J} , \qquad (A6)$$

$$\delta \equiv \delta_{11} + \delta_{22} - 2\delta_{12} . \qquad (A7)$$

The mixing parameter $\bar{\varepsilon}_J$ can subsequently be calculated from

$$\tan 2\varepsilon = \frac{2R_{12} \cos(\theta_a + \theta_b - \delta)}{R_{11} \cos 2\theta_a + R_{22} \cos 2\theta_b} , \qquad (A8)$$

where $\varepsilon \equiv \bar{\varepsilon}_J$. Next the elements of the matrix H^J are isolated. One finds

$$2 \cos 2\varepsilon\, H_{11} = R_{11} \cos 2\theta_a(1 + \cos 2\varepsilon) + R_{22} \cos 2\theta_b(1 - \cos 2\varepsilon) , \qquad (A9)$$

$$2 \cos 2\varepsilon\, H_{22} = R_{11} \cos 2\theta_a(1 - \cos 2\varepsilon) + R_{22} \cos 2\theta_b(1 + \cos 2\varepsilon) , \qquad (A10)$$

$$\cos 2\varepsilon\, H_{12} = R_{12} \sin(\delta - \theta_a - \theta_b) . \qquad (A11)$$

If the matrix H^J is parametrized according to Klarsfeld [96], the three inelastic parameters $\eta_{J-1,J}$, $\eta_{J+1,J}$, and ω_J can be obtained from

$$\eta_{J-1,J} + \eta_{J+1,J} = \mathrm{Tr}\, H^J , \qquad (A12)$$

$$\eta_{J-1,J}\eta_{J+1,J} = \det H^J , \qquad (A13)$$

$$\tan 2\omega_J = 2H_{12}/(H_{11} - H_{22}) . \qquad (A14)$$

[1] W.A. van der Sanden, A.H. Emmen, and J.J. de Swart, Nijmegen Report THEF-NYM-83.11, Nijmegen, 1983 (unpublished).

[2] R.A. Arndt, L.D. Roper, R.A. Bryan, R.B. Clark, B.J. VerWest, and P. Signell, Phys. Rev. D 28, 97 (1983).

[3] R.A. Arndt, J.S. Hyslop, III, and L.D. Roper, Phys. Rev. D 35, 128 (1987).

[4] J. Bystricky, C. Lechanoine-LeLuc, and F. Lehar, J. Phys. (Paris) 48, 199 (1987); F. Lehar, C. Lechanoine-LeLuc, and J. Bystricky, ibid. 48, 199 (1987).

[5] J.R. Bergervoet, P.C. van Campen, W.A. van der Sanden, and J.J. de Swart, Phys. Rev. C 38, 15 (1988).

[6] J.R. Bergervoet, P.C. van Campen, R.A.M. Klomp, J.-L. de Kok, T.A. Rijken, V.G.J. Stoks, and J.J. de Swart, Phys. Rev. C 41, 1435 (1990).

[7] V.G.J. Stoks, R.A.M. Klomp, M.C.M. Rentmeester, and J.J. de Swart, Phys. Rev. C 48, 792 (1993).

[8] I.L. Grach, B.O. Kerbikov, and Yu.A. Simonov, Phys. Lett. B 208, 309 (1988).

[9] J. Mahalanabis, H.J. Pirner, and T.-A. Shibata, Nucl. Phys. A485, 546 (1988).

[10] H.J. Pirner, B. Kerbikov, and J. Mahalanabis, Z. Phys. A 338, 111 (1991).

[11] E. Fett, A. Haatuft, J.M. Olsen, W. Hart, D. Waldren, P. Alibran, B. Degrange, R. Arnold, J.P. Engel, and S. de Unamuno, Nucl. Phys. B130, 1 (1977).

[12] J. Vandermeulen, Z. Phys. C 37, 563 (1988).

[13] M.P. Locher and B.S. Zou, Z. Phys. A 341, 191 (1992).

[14] J.S. Ball and G.F. Chew, Phys. Rev. 109, 1385 (1958).

[15] M.S. Spergel, Il Nuovo Cimento A 47, 410 (1967).

[16] O.D. Dalkarov and F. Myhrer, Il Nuovo Cimento A 40, 152 (1977).

[17] A. Delville, P. Jasselette, and J. Vandermeulen, Am. J. Phys. 46, 907 (1978).

[18] R.A. Bryan and R.J.N. Phillips, Nucl. Phys. B5, 201 (1968); B7, 481(E) (1968); R.J.N. Phillips, Rev. Mod. Phys. 39, 681 (1967).

[19] F. Myhrer and A. Gersten, Il Nuovo Cimento A 37, 21 (1977).

[20] C.B. Dover and J.-M. Richard, Phys. Rev. C 21, 1466 (1980); 25, 1952 (1982).

[21] M. Kohno and W. Weise, Nucl. Phys. A454, 429 (1986).

[22] T.-A. Shibata, Phys. Lett. B 189, 232 (1987).

[23] T. Hippchen, K. Holinde, and W. Plessas, Phys. Rev. C 39, 761 (1989).

[24] J. Côté, M. Lacombe, B. Loiseau, B. Moussallam, and R. Vinh Mau, Phys. Rev. Lett. 48, 1319 (1982); M. Lacombe, B. Loiseau, B. Moussallam, and R. Vinh Mau, Phys. Rev. C 29, 1800 (1984).

[25] M. Pignone, M. Lacombe, B. Loiseau, and R. Vinh Mau, Phys. Rev. Lett. 67, 2423 (1991).

[26] P.H. Timmers, W.A. van der Sanden, and J.J. de Swart, Phys. Rev. D 29, 1928 (1984).

[27] G.Q. Liu and F. Tabakin, Phys. Rev. C 41, 665 (1990).

[28] R. Timmermans, Ph.D. thesis, University of Nijmegen, The Netherlands, 1991.

[29] R. Timmermans, Th.A. Rijken, and J.J. de Swart, Phys. Rev. Lett. 67, 1074 (1991).

[30] M.M. Nagels, T.A. Rijken, and J.J. de Swart, Phys. Rev. D 17, 768 (1978).

[31] R. Timmermans, Th.A. Rijken, and J.J. de Swart, Phys. Lett. B 257, 227 (1991).

[32] R. Timmermans, Th.A. Rijken, and J.J. de Swart, Phys. Rev. D 45, 2288 (1992).

[33] M.H. Partovi and E.L. Lomon, Phys. Rev. D 2, 1999 (1970).

[34] K. Erkelenz, Phys. Rep. C 13, 191 (1974).

[35] B.A. Lippmann and J. Schwinger, Phys. Rev. 79, 469 (1950).

[36] A.A. Logunov and A.N. Tavkhelidze, Il Nuovo Cimento 29, 380 (1963).

[37] R. Blankenbecler and R. Sugar, Phys. Rev. 142, 1051

(1966).

[38] V.G. Kadyshevsky, Nucl. Phys. **B6**, 125 (1968).

[39] V.G. Kadyshevsky and M.D. Mateev, Il Nuovo Cimento A **55**, 275 (1968).

[40] E.E. Salpeter and H.A. Bethe, Phys. Rev. **84**, 1232 (1951).

[41] M. Gell-Mann and F. Low, Phys. Rev. **84**, 350 (1951).

[42] M.M. Nagels, T.A. Rijken, and J.J. de Swart, Phys. Rev. D **15**, 2547 (1977).

[43] J.J. de Swart and M.M. Nagels, Fortschr. Phys. **26**, 215 (1978).

[44] J.R. Bergervoet, Ph.D. thesis, University of Nijmegen, 1987.

[45] L. Wolfenstein and J. Ashkin, Phys. Rev. **85**, 947 (1952).

[46] N. Hoshizaki, Prog. Theor. Phys. Suppl. **42**, 107 (1968).

[47] J. Bystricky, F. Lehar, and P. Winternitz, J. Phys. (Paris) **39**, 1 (1978).

[48] P. LaFrance and P. Winternitz, J. Phys. (Paris) **41**, 1391 (1980).

[49] J. Bystricky, F. Lehar, and P. Winternitz, J. Phys. (Paris) **45**, 207 (1984).

[50] P. LaFrance, F. Lehar, B. Loiseau, and P. Winternitz, Helv. Phys. Acta **65**, 611 (1992).

[51] H. Feshbach and E.L. Lomon, Ann. Phys. (N.Y.) **29**, 19 (1964).

[52] R.L. Jaffe and F.E. Low, Phys. Rev. D **19**, 2105 (1979).

[53] R.L. Jaffe, in *Asymptotic Realms of Physics*, edited by A.H. Guth, K. Huang, and R.L. Jaffe (MIT Press, Cambridge, 1983), p. 100.

[54] B.L.G. Bakker and P.J. Mulders, Adv. Nucl. Phys. **17**, 1 (1986).

[55] J.J. de Swart, J.R.M. Bergervoet, P.C.M. van Campen, and W.A.M. van der Sanden, in *Advanced Methods in the Evaluation of Nuclear Scattering Data*, edited by H.J. Krappe and R. Lipperheide, Lecture Notes in Physics, Vol. 236 (Springer-Verlag, Berlin, 1985), p. 179.

[56] H. Feshbach, Ann. Phys. (N.Y.) **5**, 357 (1958); **19**, 287 (1962); **43**, 410 (1967).

[57] G. Breit, Phys. Rev. **99**, 1581 (1955).

[58] G.J.M. Austen and J.J. de Swart, Phys. Rev. Lett. **50**, 2039 (1983).

[59] L. Durand, III, Phys. Rev. **108**, 1597 (1957).

[60] V. Stoks, R. Timmermans, and J.J. de Swart, Phys. Rev. C **47**, 512 (1993).

[61] P.M.M. Maessen, Th.A. Rijken, and J.J. de Swart, Phys. Rev. C **40**, 2226 (1989).

[62] J.J. de Swart, T.A. Rijken, P.M. Maessen, and R. Timmermans, Il Nuovo Cimento A **102**, 203 (1989).

[63] N. Hoshizaki, I. Lin, and S. Machida, Prog. Theor. Phys. (Kyoto) **24**, 480 (1960).

[64] N. Hoshizaki, S. Otsuki, W. Watari, and M. Yonezawa, Prog. Theor. Phys. (Kyoto) **27**, 1199 (1962).

[65] R.A. Bryan and B.L. Scott, Phys. Rev. **135**, B434 (1964); **177**, 1435 (1969).

[66] J. Binstock and R.A. Bryan, Phys. Rev. D **4**, 1341 (1971).

[67] R.A. Bryan and A. Gersten, Phys. Rev. D **6**, 341 (1972).

[68] S.D. Protopopescu, M. Alston-Garnjost, A. Barbaro-Galtieri, S.M. Flatté, J.H. Friedman, T.A. Lasinski, G.R. Lynch, M.S. Rabin, and F.T. Solmitz, Phys. Rev. D **7**, 1279 (1973).

[69] M. Svec, A. de Lesquen, and L. van Rossum, Phys. Rev. D **46**, 949 (1992).

[70] M. Svec, A. de Lesquen, and L. van Rossum, Phys. Rev. D **45**, 1518 (1992).

[71] R.L. Jaffe, Phys. Rev. D **15**, 267 (1977).

[72] A.T. Aerts, P.J. Mulders, and J.J. de Swart, Phys. Rev. D **21**, 1370 (1980).

[73] S.R. Sharpe, R.L. Jaffe, and M.R. Pennington, Phys. Rev. D **30**, 1013 (1984).

[74] J.J. Engelen, M.J. Holwerda, E.W. Kittel, H.G.J.M. Tiecke, J.S.M. Vergeest, B. Jongejans, G.G.G. Massaro, H. Voorthuis, R.J. Hemingway, S.O. Holmgren, M.J. Losty, S. Yamashita, P. Grossmann, L. Lyons, and L. McDowell, Nucl. Phys. **B134**, 14 (1978).

[75] F.E. Low, Phys. Rev. D **12**, 163 (1975).

[76] S. Nussinov, Phys. Rev. Lett. **34**, 1286 (1975).

[77] Yu.A. Simonov, Phys. Lett. B **249**, 514 (1990).

[78] C.B. Dover and J.-M. Richard, Phys. Rev. D **17**, 1770 (1978).

[79] C.B. Dover and J.-M. Richard, Ann. Phys. (N.Y.) **121**, 70 (1979).

[80] W. Buck, C.B. Dover, and J.-M. Richard, Ann. Phys. (N.Y.) **121**, 47 (1979).

[81] G. Schierholz and S. Wagner, Nucl. Phys. **B32**, 306 (1971).

[82] L.N. Bogdanova, O.D. Dalkarov, and I.S. Shapiro, Ann. Phys. (N.Y.) **84**, 261 (1974).

[83] I.S. Shapiro, Phys. Rep. C **35**, 129 (1978).

[84] L. Montanet, G.C. Rossi, and G. Veneziano, Phys. Rep. **63**, 153 (1980).

[85] J. Carbonell, O.D. Dalkarov, K.V. Protasov, and I.S. Shapiro, Nucl. Phys. **A535**, 651 (1991).

[86] J.R. Taylor, Il Nuovo Cimento B **23**, 313 (1974).

[87] M.D. Semon and J.R. Taylor, Il Nuovo Cimento A **26**, 48 (1975).

[88] A. Gersten, Nucl. Phys. **B103**, 465 (1976).

[89] V.G.J. Stoks and J.J. de Swart, Phys. Rev. C **42**, 1235 (1990).

[90] L.D. Knutson and D. Chiang, Phys. Rev. C **18**, 1958 (1978).

[91] W.A. van der Sanden (unpublished).

[92] J.M. Blatt and L.C. Biedenharn, Phys. Rev. **86**, 399 (1952).

[93] H.P. Stapp, T.J. Ypsilantis, and N. Metropolis, Phys. Rev. **105**, 302 (1957).

[94] R.A. Bryan, Phys. Rev. C **24**, 2659 (1981); **30**, 305 (1984); **39**, 783 (1989).

[95] D.W.L. Sprung and M.W. Kermode, Phys. Rev. C **26**, 1327 (1982).

[96] S. Klarsfeld, Phys. Lett. **126B**, 148 (1983).

[97] D.W.L. Sprung, Phys. Rev. C **32**, 699 (1985); **35**, 869 (1987).

[98] R.A. Arndt and M.H. MacGregor, in *Methods in Computational Physics*, edited by B. Alder, S. Fernbach, and M. Rotenberg (Academic Press, New York, 1966), Vol. 6, p. 253.

[99] R.P. Hamilton, T.P. Pun, R.D. Tripp, H. Nicholson, and D.M. Lazarus, Phys. Rev. Lett. **44**, 1179 (1980).

[100] W. Brückner, B. Cujec, H. Döbbeling, K. Dworschak, F. Güttner, H. Kneis, S. Majewski, M. Nomachi, S. Paul, B. Povh, R.D. Ransome, T.-A. Shibata, M. Treichel, and Th. Walcher, Z. Phys. A **335**, 217 (1990).

[101] W. Brückner, H. Döbbeling, F. Güttner, D. von Harrach, H. Kneis, S. Majewski, M. Nomachi, S. Paul, B. Povh, R.D. Ransome, T.-A. Shibata, M. Treichel, and Th. Walcher, Phys. Lett. **166B**, 113 (1986).

[102] W. Brückner, B. Cujec, H. Döbbeling, K. Dworschak, H. Kneis, S. Majewski, M. Nomachi, S. Paul, B. Povh, R.D. Ransome, T.-A. Shibata, M. Treichel, and Th. Walcher, Z. Phys. A **339**, 367 (1991).

[103] W. Brückner, H. Döbbeling, F. Güttner, D. von Harrach, H. Kneis, S. Majewski, M. Nomachi, S. Paul, B. Povh, R.D. Ransome, T.-A. Shibata, M. Treichel, and Th. Walcher, Phys. Lett. **169B**, 302 (1986).

[104] D. Spencer and D.N. Edwards, Nucl. Phys. **B19**, 501 (1970).

[105] W. Brückner, B. Cujec, H. Döbbeling, K. Dworschak, F. Güttner, H. Kneis, S. Majewski, M. Nomachi, S. Paul, B. Povh, R.D. Ransome, T.-A. Shibata, M. Treichel, and Th. Walcher, Phys. Lett. B **197**, 463 (1987); **199**, 596(E) (1987).

[106] D.V. Bugg, J. Hall, A.S. Clough, R.L. Shypit, K. Bos, J.C. Kluyver, R.A. Kunne, L. Linssen, R. Birsa, F. Bradamante, S. Dalla Torre-Colautti, A. Martin, A. Penzo, P. Schiavon, A. Villari, E. Heer, C. LeLuc, Y. Onel, and D. Rapin, Phys. Lett. B **194**, 563 (1987).

[107] L. Linssen, C.I. Beard, R. Birsa, K. Bos, F. Bradamante, D.V. Bugg, A.S. Clough, S. Dalla Torre-Colautti, M. Giorgi, J.R. Hall, J.C. Kluyver, R.A. Kunne, C. Lechanoine-LeLuc, A. Martin, Y. Onel, A. Penzo, D. Rapin, P. Schiavon, R.L. Shypit, and A. Villari, Nucl. Phys. **A469**, 726 (1987).

[108] M. Alston-Garnjost, R. Kenney, D. Pollard, R. Ross, R. Tripp, and H. Nicholson, Phys. Rev. Lett. **35**, 1685 (1975).

[109] T. Sumiyoshi, J. Chiba, T. Fujii, H. Iwasaki, T. Kageyama, S. Kuribayashi, K. Nakamura, T. Takeda, H. Ikeda, and Y. Takada, Phys. Rev. Lett. **49**, 628 (1982).

[110] B. Conforto, G. Fidecaro, H. Steiner, R. Bizzarri, P. Guidoni, F. Marcelja, G. Brautti, E. Castelli, M. Ceschia, and M. Sessa, Il Nuovo Cimento A **54**, 441 (1968).

[111] R.P. Hamilton, T.P. Pun, R.D. Tripp, D.M. Lazarus, and H. Nicholson, Phys. Rev. Lett. **44**, 1182 (1980).

[112] M. Cresti, L. Peruzzo, and G. Sartori, Phys. Lett. **132B**, 209 (1983).

[113] S. Sakamoto, T. Hashimoto, F. Sai, and S.S. Yamamoto, Nucl. Phys. **B195**, 1 (1982).

[114] A.S. Clough, C.I. Beard, D.V. Bugg, J.A. Edgington, J. Hall, K. Bos, J.C. Kluyver, R.A. Kunne, L. Linssen, R. Birsa, F. Bradamante, S. Dalla Torre-Colautti, M. Giorgi, A. Martin, A. Penzo, P. Schiavon, A. Villari, S. Degli-Agosti, E. Heer, R. Hess, C. Lechanoine-LeLuc, Y. Onel, and D. Rapin, Phys. Lett. **146B**, 299 (1984).

[115] T. Kageyama, T. Fujii, K. Nakamura, F. Sai, S. Sakamoto, S. Sato, T. Takahashi, T. Tanimori, S.S. Yamamoto, and Y. Takada, Phys. Rev. D **35**, 2655 (1987).

[116] K. Nakamura, T. Fujii, T. Kageyama, F. Sai, S. Sakamoto, S. Sato, T. Takahashi, T. Tanimori, and S.S. Yamamoto, Phys. Rev. Lett. **53**, 885 (1984).

[117] M. Alston-Garnjost, R.P. Hamilton, R.W. Kenney, D.L. Pollard, R.D. Tripp, H. Nicholson, and D.M. Lazarus, Phys. Rev. Lett. **43**, 1901 (1979).

[118] H. Iwasaki, H. Aihara, J. Chiba, H. Fujii, T. Fujii, T. Kamae, K. Nakamura, T. Sumiyoshi, Y. Takada, T. Takeda, M. Yamauchi, and H. Fukuma, Phys. Lett. **103B**, 247 (1981).

[119] R. Bizzarri, B. Conforto, G.C. Gialanella, P. Guidoni, F. Marcelja, E. Castelli, M. Ceschia, and M. Sessa, Il Nuovo Cimento A **54**, 456 (1968).

[120] F. Perrot-Kunne, R. Bertini, M. Costa, H. Catz, A. Chaumeaux, J.-C. Faivre, E. Vercellin, J. Arvieux, J. Yonnet, B. van den Brandt, D.R. Gill, J.A. Konter, S. Mango, G.D. Wait, E. Boschitz, W. Gyles, W. List, C. Otterman, R. Tacik, and M. Wessler, Phys. Lett. B **261**, 188 (1991).

[121] T. Tsuboyama, Y. Kubota, F. Sai, S. Sakamoto, and S.S. Yamamoto, Phys. Rev. D **28**, 2135 (1983).

[122] R.A. Kunne, C.I. Beard, R. Birsa, K. Bos, F. Bradamante, D.V. Bugg, A.S. Clough, S. Dalla Torre-Colautti, S. Degli-Agosti, J.A. Edgington, J.R. Hall, E. Heer, R. Hess, J.C. Kluyver, C. Lechanoine-LeLuc, L. Linssen, A. Martin, T.O. Niinikoski, Y. Onel, A. Penzo, D. Rapin, J.M. Rieubland, A. Rijllart, P. Schiavon, R.L. Shypit, F. Tessarotto, A. Villari, and P. Wells, Phys. Lett. B **206**, 557 (1988).

[123] R.A. Kunne, C.I. Beard, R. Birsa, K. Bos, F. Bradamante, D.V. Bugg, A.S. Clough, S. Dalla Torre-Colautti, J.A. Edgington, J.R. Hall, E. Heer, R. Hess, J.C. Kluyver, C. Lechanoine-LeLuc, L. Linssen, A. Martin, T.O. Niinikoski, Y. Onel, A. Penzo, D. Rapin, J.M. Rieubland, A. Rijllart, P. Schiavon, R.L. Shypit, F. Tessarotto, A. Villari, and P. Wells, Nucl. Phys. **B323**, 1 (1989).

[124] R. Birsa, F. Bradamante, A. Bressan, S. Dalla Torre-Colautti, M. Giorgi, M. Lamanna, A. Martin, A. Penzo, P. Schiavon, F. Tessarotto, M.P. Macciotta, A. Masoni, G. Puddu, S. Serci, T. Niinikoski, A. Rijllart, A. Ahmidouch, E. Heer, R. Hess, C. Lechanoine-LeLuc, C. Mascarini, D. Rapin, J. Arvieux, R. Bertini, H. Catz, J.C. Faivre, R.A. Kunne, F. Perrot-Kunne, M. Agnello, F. Iazzi, B. Minetti, T. Bressani, E. Chiavassa, N. De Marco, A. Musso, and A. Piccotti, Phys. Lett. B **273**, 533 (1991).

[125] P. Schiavon, R. Birsa, K. Bos, F. Bradamante, A.S. Clough, S. Dalla Torre-Colautti, J.R. Hall, E. Heer, R. Hess, J.C. Kluyver, R.A. Kunne, C. Lechanoine-LeLuc, L. Linssen, A. Martin, Y. Onel, A. Penzo, D. Rapin, R.L. Shypit, F. Tessarotto, and A. Villari, Nucl. Phys. **A505**, 595 (1989).

[126] R. Birsa, F. Bradamante, S. Dalla Torre-Colautti, M. Giorgi, M. Lamanna, A. Martin, A. Penzo, P. Schiavon, F. Tessarotto, M.P. Macciotta, A. Masoni, G. Puddu, S. Serci, T. Niinikoski, A. Rijllart, A. Ahmidouch, E. Heer, R. Hess, R.A. Kunne, C. Lechanoine-LeLuc, C. Mascarini, D. Rapin, J. Arvieux, R. Bertini, H. Catz, J.C. Faivre, F. Perrot-Kunne, M. Agnello, F. Iazzi, B. Minetti, T. Bressani, E. Chiavassa, N. De Marco, A. Musso, and A. Piccotti, Phys. Lett. B **246**, 267 (1990).

[127] T. Ohsugi, M. Fujisaki, S. Kaneko, Y. Murata, K. Okamura, H. Kohno, M. Fukawa, R. Hamatsu, T. Hirose, S. Kitamura, T. Mamiya, T. Yamagata, T. Emura, I. Kita, and K. Takahashi, Il Nuovo Cimento A **17**, 456 (1973).

[128] E. Eisenhandler, W.R. Gibson, C. Hojvat, P.I.P. Kalmus, L.C.Y. Lee, T.W. Pritchard, E.C. Usher, D.T. Williams, M. Harrison, W.H. Range, M.A.R. Kemp, A.D. Rush, J.N. Woulds, G.T.J. Arnison, A. Astbury, D.P. Jones, and A.S.L. Parsons, Nucl. Phys. **B113**, 1 (1976).

[129] H. Kohno, S. Kaneko, Y. Murata, T. Ohsugi, K. Okamura, M. Fukawa, R. Hamatsu, T. Hirose, T. Mamiya, T. Yamagata, T. Emura, I. Kita, and K. Takahashi, Nucl. Phys. **B41**, 485 (1972).

[130] R. Bertini, M. Costa, F. Perrot, H. Catz, A. Chaumeaux, J.Cl. Faivre, E. Vercellin, J. Arvieux, J. Yonnet, B. van den Brandt, J.A. Konter, D.R. Gill, S. Mango, G.D. Wait, E. Boschitz, W. Gyles, W. List, C. Otterman, R. Tacik, M. Wessler, E. Descroix, J.Y. Grossiord, and A. Guichard, Phys. Lett. B **228**, 531 (1989).

[131] M. Kimura, M. Takanaka, R. Hamatsu, Y. Hattori, T. Hirose, S. Kitamura, T. Yamagata, T. Emura, I. Kita, K. Takahashi, H. Kohno, and S. Matsumoto, Il Nuovo Cimento **71A**, 438 (1982).

[132] M.G. Albrow, S. Andersson-Almehed, B. Bošnjaković, C. Daum, F.C. Erné Y. Kimura, J.P. Lagnaux, J.C. Sens, and F. Udo, Nucl. Phys. **B37**, 349 (1972).

[133] A.S. Carroll, I-H. Chiang, T.F. Kycia, K.K. Li, P.O. Mazur, D.N. Michael, P. Mockett, D.C. Rahm, and R. Rubinstein, Phys. Rev. Lett. **32**, 247 (1974).

[134] V. Chaloupka, H. Dreverman, F. Marzano, L. Montanet, P. Schmid, J.R. Fry, H. Rohringer, S. Simopoulou, J. Hanton, F. Grard, V.P. Henri, H. Johnstad, J.M. Lesceux, J.S. Skura, A. Bettini, M. Cresti, L. Peruzzo, P. Rossi, R. Bizzarri, M. Iori, E. Castelli, C. Omero, and P. Poropat, Phys. Lett. **61B**, 487 (1976).

[135] S. Sakamoto, T. Hashimoto, F. Sai, and S.S. Yamamoto, Nucl. Phys. **B158**, 410 (1979).

[136] T. Kamae, H. Aihara, J. Chiba, H. Fujii, T. Fujii, H. Iwasaki, K. Nakamura, T. Sumiyoshi, Y. Takada, T. Takeda, M. Yamauchi, H. Fukuma, and T. Takeshita, Phys. Rev. Lett. **44**, 1439 (1980).

[137] K. Nakamura, H. Aihara, J. Chiba, H. Fujii, T. Fujii, H. Iwasaki, T. Kamae, T. Sumiyoshi, Y. Takada, T. Takeda, M. Yamauchi, H. Fukuma, and T. Takeshita, Phys. Rev. D **29**, 349 (1984).

[138] P.H. Timmers, W.A. van der Sanden, and J.J. de Swart, Phys. Rev. D **31**, 99 (1985).

[139] W. Brückner, B. Granz, D. Ingham, K. Kilian, U. Lynen, J. Niewisch, B. Pietrzyk, B. Povh, H.G. Ritter, and H. Schröder, Phys. Lett. **67B**, 222 (1977).

[140] E. Jastrzembski, N. Haik, W.K. McFarlane, M.A. Mandelkern, D.C. Schultz, C. Amsler, C.C. Herrmann, and D.M. Wolfe, Phys. Rev. D **23**, R2784 (1981).

[141] D.I. Lowenstein, D.C. Peaslee, C. Bromberg, R.A. Lewis, R. Miller, B.Y. Oh, T. Potter, G.A. Smith, J. Whitmore, T. Brando, T.E. Kalogeropoulos, G. Onengut, C. Petridou, M. Singer, and G.S. Tzanakos, Phys. Rev. D **23**, R2788 (1981).

[142] F. Sai, S. Sakamoto, and S.S. Yamamoto, Nucl. Phys. **B213**, 371 (1983).

[143] T. Brando, I. Daftari, A. Deguzman, T.E. Kalogeropoulos, R.A. Lewis, D.I. Lowenstein, R.J. Miller, B.Y. Oh, D.C. Peaslee, C. Petridou, M. Singer, G.A. Smith, G.S. Tzanakos, R. Venugopal, R.D. von Lintig, and J. Whitmore, Phys. Lett. **158B**, 505 (1985).

[144] J. Franklin, Phys. Lett. B **184**, 111 (1987).

[145] M. Coupland, E. Eisenhandler, W.R. Gibson, P.I.P. Kalmus, and A. Astbury, Phys. Lett. **71B**, 460 (1977).

[146] H. Kaseno, Il Nuovo Cimento A **43**, 119 (1978).

[147] V. Ashford, M.E. Sainio, M. Sakitt, J. Skelly, R. Debbe, W. Fickinger, R. Marino, and D.K. Robinson, Phys. Rev. Lett. **54**, 518 (1985).

[148] W. Brückner, H. Döbbeling, F. Güttner, D. von Harrach, H. Kneis, S. Majewski, M. Nomachi, S. Paul, B. Povh, R.D. Ransome, T.-A. Shibata, M. Treichel, and Th. Walcher, Phys. Lett. **158B**, 180 (1985).

[149] W. Brückner, B. Cujec, H. Döbbeling, K. Dworschak, H. Kneis, S. Majewski, M. Nomachi, S. Paul, B. Povh, R.D. Ransome, T.-A. Shibata, M. Treichel, and Th. Walcher, Z. Phys. A **339**, 379 (1991).

[150] R.A. Kunne, C.I. Beard, R. Birsa, K. Bos, F. Bradamante, D.V. Bugg, A.S. Clough, S. Dalla Torre-Colautti, J.A. Edgington, M. Giorgi, J.R. Hall, E. Heer, R. Hess, J.C. Kluyver, C. Lechanoine-LeLuc, L. Linssen, A. Martin, T.O. Niinikoski, Y. Onel, A. Penzo, D. Rapin, J.M. Rieubland, A. Rijllart, P. Schiavon, R.L. Shypit, F. Tessarotto, and A. Villari, Phys. Lett. B **261**, 191 (1991).

[151] M. Bogdanski, T. Emura, S.N. Ganguli, A. Gurtu, S. Hamada, R. Hamatsu, E. Jeannet, I. Kita, S. Kitamura, J. Kishiro, H. Kohno, M. Komatsu, P.K. Malhorta, S. Matsumoto, U. Mehtani, L. Montanet, R. Raghavan, A. Subramanian, K. Takahashi, and T. Yamagata, Phys. Lett. **62B**, 117 (1976).

[152] S. Banerjee, S.N. Ganguli, A. Gurtu, P.K. Malhorta, R. Raghavan, A. Subramanian, K. Sudhakar, M.M. Agarwal, J.M. Kohli, J.P. Lamba, I.S. Mittra, J.B. Singh, P.M. Sood, Dev Anand, P.V.K.S. Baba, G.L. Kaul, Y. Prakash, N.K. Rao, G. Singh, R. Hamatsu, T. Hirose, S. Kitamura, and T. Yamagata, Z. Phys. C **28**, 163 (1985).

[153] M.P. Macciotta, A. Masoni, G. Puddu, S. Serci, A. Ahmidouch, E. Heer, C. Mascarini, D. Rapin, J. Arvieux, R. Bertini, J.C. Faivre, R.A. Kunne, R. Birsa, F. Bradamante (Spokesman), A. Bressan, S. Dalla Torre-Colautti, M. Giorgi, M. Lamanna, A. Martin, A. Penzo, P. Schiavon, F. Tessarotto, A.M. Zanetti, E. Chiavassa, N. De Marco, A. Musso, and A. Piccotti, PS199 Collaboration, CERN Report CERN/SPSLC 92-17, 1992.

[154] E. Leader, Phys. Lett. **60B**, 290 (1976).

[155] R.A.M. Klomp, V.G.J. Stoks, and J.J. de Swart, Phys. Rev. C **44**, R1258 (1991).

[156] R.A. Arndt, Z. Li, L.D. Roper, and R.L. Workman, Phys. Rev. Lett. **65**, 157 (1990).